Moving Object Pipeline System Design

Jonathan Myers, Lynne Jones, Tim Axelrod

ABSTRACT

The Moving Object Pipeline System (MOPS) has two responsibilities within LSST Data Management. First, it is responsible for generating and managing the **Moving Object** data products. The Moving Objects are identified solar system objects with associated Keplerian orbits, errors, and detected sources associated with those solar system objects. The second responsibility of the MOPS is to predict future locations of moving objects in incoming images so that their sources may be associated with known objects; this will reduce the number of transient detections and prevent Alert Generation on detections of known Solar System objects.

Contents

List of Figures

1.   Overview

The Moving Object Pipeline System has two main responsibilities: the generation and maintenance of the Moving Object database (*i.e.*. the discovery and linking of all observations of each moving object), and the prediction of known object locations which are sent to the Alert Pipeline to prevent unneccessary alerts. To serve these two functions, MOPS operates in two components, known as "DayMOPS" and "NightMOPS."

"NightMOPS" (operating throughout each night) is responsible for predicting the locations of known Moving Objects in upcoming images. This is intended solely to help flag known moving objects in the LSST alert stream. "DayMOPS" (operating after each night's data is complete, typically in the day) is responsible for discovering new Moving Objects in newly-acquired data, searching old data for detections of new objects ('precovery), identifying known moving objects in newly-acquired data ('attribution') and updating the Moving Objects database. Note that 'attribution' is distinct from NightMOPS, as attribution can take advantage of additional information coming from observations throughout the entire night, allowing matches between new detections and moving objects under larger positional uncertainties, and also folds this information back into the Moving Object database. DayMOPS is also responsible for periodically refining the contents of the Moving Objects database based on the orbits of the known objects.

The relationship between NightMOPS, DayMOPS, and the neighboring components of the LSST Data Management system is illustrated in figure 1.
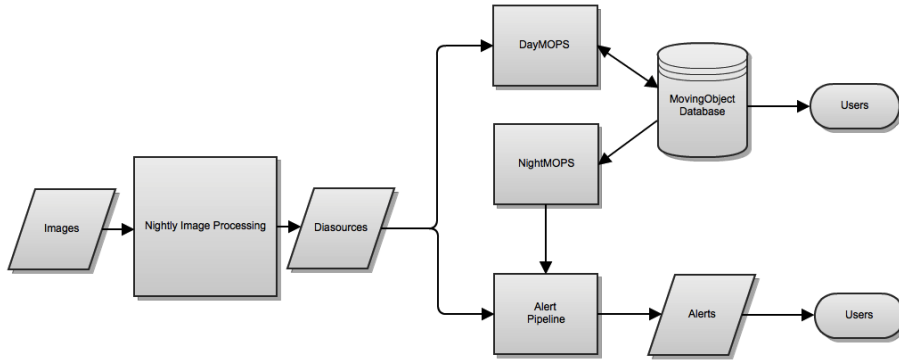

Fig. 1.—: Data flow within LSST, from image acquisition to the Moving Object database and Alert generation. DayMOPS will build and maintain the Moving Objects table, NightMOPS will use the Moving Objects table to predict positions of known moving objects and communicate with the Assocation Pipeline.

1.1. NightMOPS: Serving the Alert stream

1.1.1. Overview

NightMOPS is a much simpler system than DayMOPS, so will be described briefly and then not discussed further in this document. The goal of NightMOPS is simply to hand the alert pipeline the information needed to flag diaSource detections (detections from each individual image, differenced against a template image) with their probability of corresponding to a known moving object. The relevant pieces of information are the names (or ID numbers) of each of the known objects in the field, their locations and expected magnitudes along with the uncertainties in these parameters, and potentially velocity vectors if visible trailing could be expected over a 30 s exposure. Joining these pieces of information to the diaSources reported in each visit is the job of the alert pipeline, and in particular, the association pipeline.

As the alert pipeline must issue alerts within 60 s of the shutter closing on each image, speed in generating the ephemerides of the objects visible in each field as it is observed is paramount. Later during the LSST survey, we expect to have on the order of 11 million known moving objects, mostly Main Belt asteroids. The orbits of these known objects can potentially change during the day if DayMOPS discovers new objects or links more detections into previously known orbits.

The general idea here is to propagate all of the known orbits to the start (or middle) of the night and generate 'coarse ephemerides' on a time grid that covers most of the night at fairly large intervals, before the night's observing begins. As individual visits are acquired during the night, these coarse ephemerides are used to generate a list of moving objects which could potentially be visible in the visit. A 'precise' ephemeris (the location, magnitude, velocity vector and uncertainties) is then generated for the exact time of the visit, for each of the moving objects which could be visible. The subject of ephemeris generation is discussed in Chapter 4, in connection with orbit determination software.

1.1.2. Status Summary

There is currently an implementation of NightMOPS in the LSST codebase which was exercised in DC2, but we expect this code to be overhauled and updated before first light, for several reasons:

- the current version of NightMOPS was written before significant upgrades to the python interface to OpenOrb (the software used to generate ephemerides),

- there has been ongoing work at UW on methods to generate ephemerides for our catalog simulations, some of which might be taken advantage of to speed up this ephemeride generation, (particularly relating to translating from coarse ephemerides to the precise ephemerides),

- it seems entirely likely that our ephemeris generation software will change before first light, given that OpenOrb is a Fortran program,

- changes in the LSST middleware will require updates to the current implementation of NightMOPS, which was developed under an older API.

1.2. DayMOPS: Discovering and Managing Moving Objects

1.2.1. Overview

DayMOPS makes up the bulk of the moving object software. It is responsible for discovering new moving objects in our data, extending the orbital arc of our known and newly discovered moving objects both backward and forward in time ('precovery' and 'attribution'), and updating the Moving Object Database with this information.

The design of LSST DayMOPS is based on (although only roughly similar to the current implementation of) the PanSTARRS Moving Object Pipeline System (Denneau et al. 2007). The approach used here is to link detections (RA/Dec measurements of non-stationary objects - in LSST these are called 'diaSources') with sky-plane paths generally consistent with asteroid behaviour. After linkage, orbit determination is used to separate true moving objects from random, roughly-but-not-quite-correct alignments.

The linking methods used are based on a tiered approach. First, two or more detections from a single night are linked into **tracklets**, under the assumption that within a short time period (we use 90 minutes as an upper limit based primarily on computational resources) all solar system objects' motions will appear linear. Thus tracklets have position and velocity, but no acceleration. Once tracklets are generated for a series of nights, they are then linked in a second stage into **tracks**. Tracks consist of detections from multiple nights, which to first order display quadratic motion across the sky, thus tracks have a position, velocity, and acceleration. The approximation that moving objects follow quadratic motion starts to break down over longer time periods, thus we limit our tracks to a time span of between 15–30 days. A set of algorithms to implement this tiered approach for the discovery of sky-plane tracks in dense data are presented in Kubica et al. (2005); these algorithms are the basis of the linking methods for the current LSST DayMOPS.

This quadratic motion assumption is used in PanSTARRS MOPS, and is a good first approximation, as virtually all objects for which a true (correctly-linked) track could be generated will actually generate a track. However, we have found that at the deeper magnitude limits of LSST, the density of moving objects is high enough that this assumption permits too many mislinkages or 'false tracks' where detections from one moving object are joined with detections from a different moving object (or other random diaSource), driving the compute costs too high. As a result, our methods diverge from those of PanSTARRS as we introduce some more strict filters (based on the chi-squared probability) and a higher-order fit on tracks, reducing the number of mislinkages at the expense of potentially missing some true tracks. The algorithms, their implementations, the additional filters, and their behaviors are presented thoroughly in Chapter 2.

Once tracks are discovered, the orbit determination phase is used to separate true linkages from mislinkages of moving objects and/or noise. The orbit determination phase takes tracks (which are just sets of diaSources which follow a roughly appropriate sky-plane path) and attempts to find a Keplerian orbit which could generate the detections. In general terms, six detections spread over three nights are sufficient to determine a preliminary (and, depending on the type of object, perhaps having rather large uncertainties) orbit – at least two detections on each night are preferred to unmistakably identify a moving object, and three night's worth of detections are needed to determine the six parameters which make up an orbit.

Initial orbit determination is the first step in orbital determination, and is where the mislinkages will fail. During differential correction, the initial orbit is further refined and error bounds are established. The process of orbit determination will reject many tracks as false, but should successfully find precise orbits for virtually all correctly linked tracks. Several methods for performing this task are known, and several have open-source implementations available to LSST (Milani et al. 2004), (Milani et al. 2006), (Granvik et al. 2009), (Granvik 2007). The orbits discovered by orbit determination and the diaSources present in the track associated with each orbit are used to generate new Moving Objects. More information on orbit fitting is presented in Chapter 4.

It is worth noting that we have chosen to follow PanSTARRS and store moving object orbital elements in cometary format; that is, perihelion distance (q), eccentricity (e), inclination (i), longitude of ascending node (node or Ω), argument of perihelion (ω) and time of perihelion (T_{peri}). For bound orbits these can be easily transformed from q and e to semi-major axis (a) while T_{peri} can be translated to mean anomaly (M), but this representation also allows expression of orbital elements for objects which appear on hyperbolic orbits such as comets.

After an orbit has been established for an object (*i.e.* a new Moving Object has been created), the observational arc of the orbit should be extended by adding earlier observations (if the object was observed earlier, but not frequently enough to generate an orbit, for example) and adding later observations as they are acquired. For MOPS, these extensions are best handled by searching for potential matching tracklets (tracklets providing a stronger constraint than single images, thus enabling cleaner matches where positional uncertainties are high or SNR may be low). The process of searching through old data is called 'Precovery'; checking incoming new data is 'Attribution'. In both cases, the new diaSources must be combined with the previously linked diaSources and a new orbit produced. Residuals in the orbit can be used to reject outliers and refine the orbit.

If there are no recoveries of a particular moving object for a period of time, ephemeris uncertainties may grow large enough to prevent further attribution. At this point, the same moving object could actually be rediscovered if it is observed with the right cadence, resulting in new moving object that would be similar (but likely not quite the same due to orbital uncertainties) to the first moving object. To account for this, DayMOPS will also periodically have to update all orbits, attempting to fit joined orbits to similar moving objects and merging these objects where the residuals in these joined fits are appropriate.

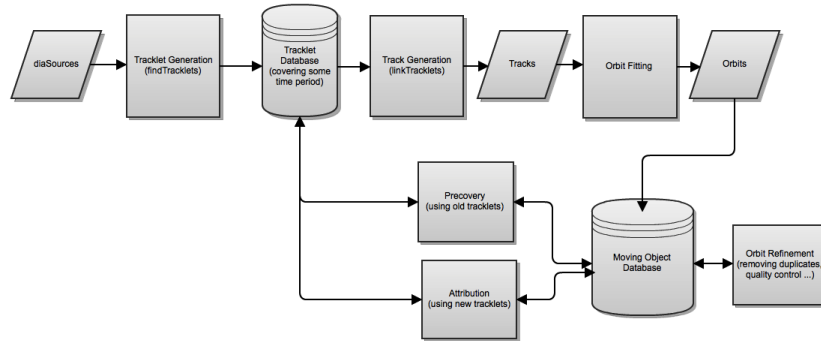The complete set of DayMOPS tasks and their data flows are illustrated in figure 2.

Fig. 2.—: Data flows into the DayMOPS pipeline and results in modifications of the Moving Objects database in a variety of ways, including attribution to known objects, a multi-stage pipeline for the discovery of new objects, and periodic refinements of the Moving Object table, such as possible merges of redundant objects or removal of false orbits.

1.2.2. Status Summary

Most of the work on dayMOPS so far has focused on the linking phases, as these are essentially the base of the computational pyramid. Chapter 2 provides a summary of the current software status. Chapter 3 describes tests which have been done with this software, including computing resource requirement estimates. Both of these chapters include small descriptions of some issues (marked with a comment as 'Issue'), but most of the software development tasks still to be done are described in more depth in Chapter 6. Many of the current outstanding issues have to do with potential geometry problems in collapseTracklets and linkTracklets, and the differences between the software implementation of RA/Dec movement compared to great-circle movements on the sky. In general, these issues need further evaluation to determine their impact, and then potentially some changes to the code. The primary impact here is likely to be to the linkTracklets code, potentially in requiring a different implementation of the KD-Tree and potentially in requiring some reworking of the equations determining compatibility. Neither of these should be hugely significant issues in themselves, especially as the KD-Tree implementation should be updated to address memory bloat and to fold in improvements in memory footprint and speed of use that may be available from tree algorithms in other LSST code such as astrometry.net and the association pipeline. The major outstanding software issue is that linkTracklets is currently too slow to run in the daytime window available to it; improvements will be needed before LSST's first light. Some experiments with parallel versions of this software are presented in Chapter 3, showing what may be possible with large-shared-memory parallel machines, but even on this hardware linkTracklets is currently too slow to run on a typical LSST cadence with large false-positive diaSource detection rates within 24 hours. It seems likely that upgrading the underlying KD-Tree algorithms will address much of the speed requirements. The major outstanding science issues are that due to resource limitations we are not searching for very fast-moving NEOs (using a limit of 0.5 deg/day in velocity) and that we are not discovering about 25% of the moving objects we are capable of. Increasing our search velocity and acceleration limits seems likely to happen hand-in-hand with improving the speed of linkTracklets overall, but discovering the reasons for not detecting all of the moving objects we should be finding will require more in-depth evaluation of the linking stages performance.

A summary of LSST's current status with regards to orbit fitting and ephemeris generation software is given in Chapter 4. The take-away here is that we have two open-source software solutions available, but neither is ideal for LSST's use in production. LSST should consider partnering with an organization to develop orbital software that will be appropriate for our future use, or may end up having to develop software in-house (prefer to avoid this).

The emphasis on linking and the lack of orbit fitting software means that very little

to no software development has been done for LSST in the areas relating to precovery and attribution or towards software for maintaining the movingObject database. These pieces of software have been developed for PanSTARRS, and we should build on the available code as possible for LSST. We should also consult with the Minor Planet Center and other knowledgable members of the community for recommendations on orbit updates (when to update an orbit, when to consider new observations as belonging to the same movingObject). Work on precovery and attribution will need integration with the database teams, as precovery and attribution are heavy catalog/database use cases. It is worth noting that precovery and attribution need to be added to the LSST compute model, as does maintaining some form of the Tracklets database over some limited timeframe around the current observing date. More information on the precovery and attribution stages is presented in Chapter 5.

The needs of the solar system science collaboration for access to an up-to-date orbit database, vs the Data Release database, and how to reconcile these two versions of the database after data release are also topics to be considered. Refinement of the movingObject orbital database (to account for later rediscoveries of the same underlying object) has not been addressed for LSST, although basic algorithms were created for PanSTARRS. Additional complications due to binary objects or planetary satellites have also not been addressed, but are generally expected to be secondary level problems.

2. The Linking Stages of DayMOPS

Sufficiently bright moving objects which are observed by the LSST telescope will generate diaSource detections, stored in the LSST diaSource detection catalog. The LSST diaSource detection catalog will also hold detections from a variety of non-moving object sources, including transient phenomena and artifacts of image processing. One of the major responsibilities of dayMOPS is to link these diaSources into tracklets and tracks, as described earlier (see Section 1.2.1).

2.1. Linear and Quadratic and more: Models of Motion
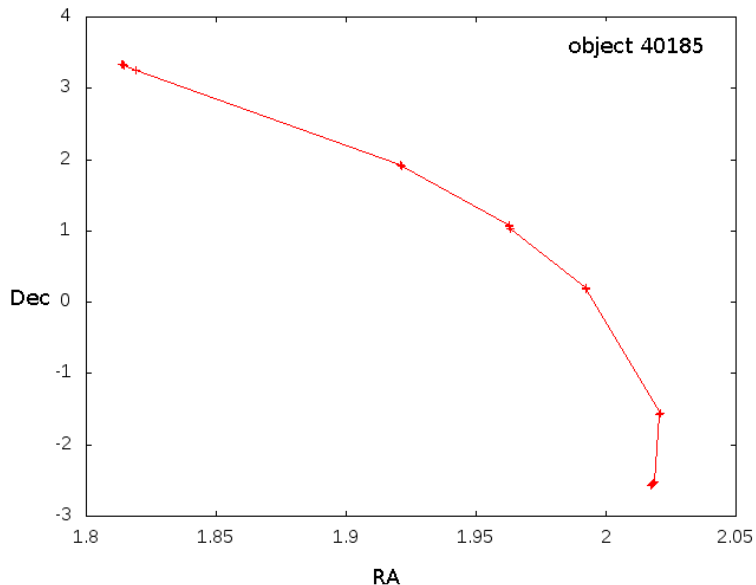
Fig. 3.—: A plot of simulated observations of object 40185 on the sky. Though the observations span only one week, a pronounced quadratic path is visible. Note that the object is observed two or more times on each night.

In order to discover and identify new objects, astronomers have traditionally used sky-plane approximations to predict and model the behavior of solar system objects for which a true orbit is not yet known. As a general rule of thumb, objects are said to move linearly (with a more or less fixed velocity) in RA and Dec over the course of a single night and quadratically (having velocity and some acceleration) in RA and Dec over the course of a month. These are, of course, approximations, and linear and quadratic fits will inevitably contain some error. An example of one object with a clear quadratic path over seven days

is show in Figure 3.

In general, these approximations become closer to the actual sky-plane motion of the object as objects are observed at larger distances from the Earth or at solar elongations closer to opposition. It's worth noting however, that for faster moving objects such as NEOs or objects observed further from opposition, these approximations start to break down; for example, NEOs do show acceleration over the course of a night (although generally not significant acceleration over 90 minutes) and any moving object near turn-around (where its motion appears to reverse direction on the sky) will provide a poor fit to quadratic motion over a month.

These basic approximations are our starting point and are used to determine which detections could plausibly be linked. For tracklets, this is simple; diaSources which can be linked with linear motion become tracklets. For tracks, however, first we determine which diaSources could potentially be joined into tracks (using the velocity information from the tracklets along the way) using quadratic motion, but then this track undergoes some further scrutiny before being marked as 'valid'.

When we are determining the validity of tracks, by looking at residuals between the observed positions and the quadratic approximation of motion (and rejecting detections or whole tracks which do not have low enough residuals), we have found that allowing for residuals high enough to account for errors due to the quadratic approximation itself permits too many mislinkages. The discovery rate of false tracks is hundreds of times the rate of discovering true tracks; we become swamped with false detections.

To avoid this, when determining the validity of a track, we now require stricter tests. The primary goal here is to reduce the residuals to allow for tighter filtering of the potential tracks. The first step is to attempt to add a topocentric correction to the detections; during the night, as the Earth rotates, objects which are close to Earth will have some additional 'wiggle' in their motion due to the change in observer's location. The topocentric correction fits the range (1/distance) of the object from the tracklet, and applies a correction to the RA locations of the tracklets that alter the observed (topocentric) values to equivalent geocentric values. The Dec values are left unchanged, as this primarily effects the RA. The second step is to attempt to fit a higher-order polynomial to the resulting RA and Dec values. If a higher-order than quadratic polynomial can be supported for the track, (*i.e.* if the fit residuals are lower than all of the errors between the predicted positions and the measured positions, the order of the fit is too high), then this higher order fit is done. After the fit for the track is created (either quadratic or higher order, potentially with a topocentric correction, but always separately fit in RA/Dec), then a chi-squared probability is computed for the track. We reject tracks with chi-squared values larger than a predetermined cutoff; this cutoff is

determined experimentally to optimize the true / false track ratio.

Note that tracklets and tracks represent hypothetical linkages, many of which may be incorrect. The linking algorithms are greedy, and intended to permit finding as many moving objects as possible. Thus, a single detection may exist in several tracklets and/or several tracks and a given tracklet may be found in multiple tracks, shown in Figure 4. However, once a diaSource is linked into an actual Orbit, it will not be joined into any further tracklets or tracks or other moving objects.
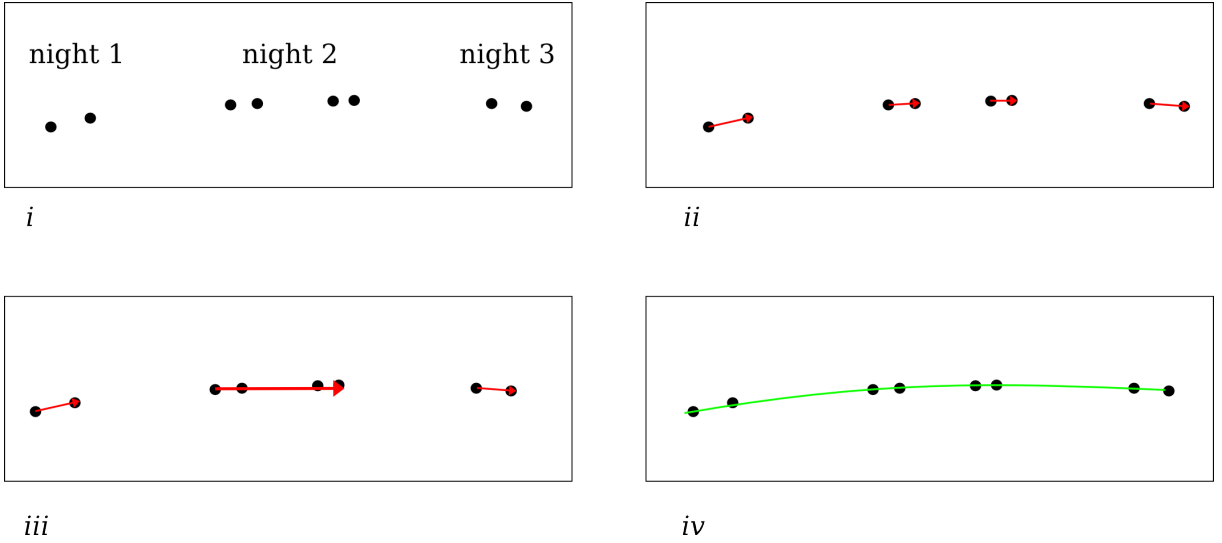
Fig. 4.—: An illustration of how DayMOPS linkage might be applied to a single object. In *i*, the object is observed on three nights; on the first and last night, it gets two detections per night, but on the second night it gets four. In *ii*, initial tracklets are generated; time separation of visits on the second night is such that we get two tracklets. In *iii*, we merge the tracklets from the second night so there are only three tracklets. In *iv*, we attempt inter-nightly linking and generate a single track.

2.2. Building Tracklets : findTracklets

Tracklets are linkages between DiaSource detections occuring within the same night. By creating tracklets, DayMOPS can find sky-plane position and velocity estimates for sets of detections which may belong to the same solar system objects. The use of tracklets also simplifies the downstream work of track generation, which attempts to find sets of detections with a good position/velocity/acceleration fit on the sky-plane; since tracklets have known position and velocity, the track generation phase needs only to find those tracklets compatible

within some acceleration factor.

Correctly-linked tracklets from a given object are needed to generate a good track for that object and eventually discover its orbit. However, if these useful tracklets are too deeply buried among very large numbers of other tracklets, then the job of tracklet linking will become extremely slow and expensive. Generally, these other, unwanted tracklets are false tracklets (mislinkages between detections not attributable to the same object), though in special conditions large numbers of correctly-linked but redundant tracklets can cause pain as well (this will discussed in 2.3).

In order to ensure that tracklet-generating images are acquired, it is necessary to ensure that fields of the sky are visited two or more times within an accepted time period each night. To constrain the number of tracklets, we impose a maximum apparent velocity on the tracklets, and also require that sky fields be revisited within a fairly short time period (≤ 90 minutes is the current rule). Raising the maximum velocity threshold enables one to find faster-moving objects, and raising the maximum allowed revisit time also enables one to generate tracklets in more fields of the sky; however, increasing either of these thresholds also increases the search space and can significantly increase the number of mislinked tracklets, greatly increasing the cost downstream.

The process of initial tracklet creation is accomplished by the findTracklets software. Later refinement of tracklets is accomplished by collapseTracklets and additional filters, primarily purifyTracklets.

2.2.1. Algorithm

The findTracklets software is responsible for finding pairs of detections which occur within a fixed time threshold, and have apparent velocity below a given threshold. For a given detection and a set of image times, one can calculate the maximum distance an object could have travelled at each time using the velocity limit. To find detections with which the query detection could be linked, one can imagine searching a circular region in the later images based on this distance.

This can be accomplished in a fairly straightforward way through the use of KD-Trees. KD-Trees are hierarchical data structures which allow for quickly and efficiently performing range searches on points in space (Bentley 1975). We use KD-Trees for many different purposes in MOPS, but what these uses have in common is exploiting the hierarchical nature of the trees; using the fact that by checking the boundaries at a high-level on a branch we may rule out having to compare any of the data stored at lower levels on that branch.
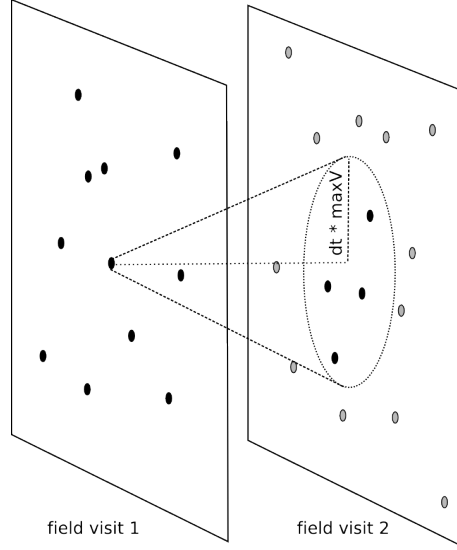
Fig. 5.—: An example of searching for compatible second endpoints for a given detection. The first detection and each of the second endpoints will be used to create a new tracklet.

A KD-Tree-based method for building tracklets was first contributed by Jeremy Kubica for his PhD thesis (Kubica 2005). For findTracklets, 2-Dimensional KD-Trees are used, covering the space of (RA, Dec). Given a detection and trees containing detections from later images, we can use range searches to quickly find nearby detections in those later images and use them for the creation of tracklets.

Because the sky is a sphere, notions of 'distance' and 'velocity' must be handled carefully, especially near the poles. Both the KD-Tree library used and the findTracklets software use actual great-circle distance and velocity for their queries, avoiding problems near the poles. The software should also be impervious to wrap-around errors - objects which move between, say, 359.9° in RA and .01° in RA will be detected. The Appendix B explains the KD-Tree library used in greater detail.

The findTracklets software itself only finds pairs of diaSources which could potentially be moving objects; if particular solar system object was observed four times in one night, it could potentially generate six separate tracklets, depending on the time of the observations and the time limits imposed by findTracklets.

2.3. Merging Tracklets

Finding multiple tracklets for a single object makes later stages of linking inefficient; if every object was observed four times per night, the number of tracklets could be increased by a factor of six - at both the start and endpoints of the tracks - resulting in a 36 times increase in the number of output tracks. Observing fields of the sky (and thus, generating multiple tracklets) more than twice in a night is common with our current OpSim runs, and is actually desireable for several purposes. In addition, the 'Deep Drilling' fields observe fields many more than twice per night. In fields observed n times per night, the number of tracklets can grow like $O(n^2)$, potentially generating huge numbers of tracklets. Merging tracklets these tracklet pairs, as appropriate, removes the inefficiencies for later stages of linking, thus there are some post-findTracklets merging and filtering stages to address this issue.

The 'collapseTracklets' software attempts to join colinear 2-detection tracklets into longer (3 detections or more) tracklets, while the 'purifyTracklets' software attempts to avoid the risk of merging mislinked with true tracklets.

In addition, it is sometimes possible that a tracklet may link together a set of detections already present in another higher cardinality (longer) tracklet; the 'removeSubsets' software finds and removes these shorter subsets. The subset removal algorithm can be used for tracks as well as tracklets, and so is presented in section 2.5 after the description of linkTracklets.

2.3.1. CollapseTracklets

In collapseTracklets, a method similar to the Hough transform is used to identify roughly colinear tracks and merge them. An intermediate time, t_c is selected (we use the average time of the first and last detections) and use the apparent linear motion of the tracklets to project their location at t_c. We then store these projected (RA,Dec) locations and the angle/velocity of each tracklet. At this point, colinear tracklets should have similar positions and motion vectors, making them easy to find. This is accomplished with a series of range searches, which of course can be implemented with 4-D (RA, Dec, angle, velocity) KD-Trees. The full pseudo-code is presented in Figure 7.

More information on collapseTracklets is available in Jon Myer's Master's thesis, titled 'Methods for Solar System Object Searching in Deep Stacks', submitted 2008 to the Dept of Computer Science at U of Arizona. A PDF of this document is available in the LSST git repository of dayMOPS/docs.

Code and usage: The collapseTracklets algorithm is implemented in `collapseTracklets.h` and `collapseTracklets.cc`. A command-line interface is implemented in `collapseTrackletsMain.cc`. Run `collapseTracklets -h` for usage hints.

Issue: Currently, collapseTracklets handles wrap-around, but otherwise treats the sky as a flat (RA, Dec) plane when calculating the projected positions of tracklets. This is acceptable for tracklets close to the ecliptic, but not sufficient closer to the poles. This should be fixed when possible.

Issue: Choosing an appropriate set of thresholds for collapseTracklets may be difficult; with variable time between images, the amount of error on velocity may differ from tracklet to tracklet. Other factors come into play as well; higher thresholds will lead to more correct linkages as well as more incorrect linkages - which, as described in the following section, can be "undone" later by purifyTracklets. We arrived at our current thresholds through simple trial and error. These threshholds will have to be evaluated for use with real data with real astrometric errors and time variability.

2.3.2. PurifyTracklets

PurifyTracklets examines the merged tracklets and removes detections if they are sufficiently far from the best-fit line. The algorithm is presented in Figure 8.

2.4. Building Tracks: linkTracklets

With tracklets already assembled, we should have many linkages representing the position, location, and velocity of the various objects observed, as well as "false" mislinked tracklets. While tracklets have only linear motion, tracks have more complex paths; in the track building phase, this is always calculated as a pair of quadratic functions in RA and Dec, rather than a single motion vector. By making use of this quadratic approximation of motion, valid for approximately one month, we can move a sliding window of up to 30 days over the data, looking for tracklets which could be linked by some quadratic acceleration factor. As we find these linkages, depending on the detections themselves (the number and timespan of detections, the best-fit distance to each object (based on the tracklet velocity), their astrometric errors) we will also apply a topocentric correction to the detections and a higher-order fit in order to apply a stronger requirement on the residuals to the fit when outputting tracks.

Generally, the track generation phase is the most computationally resource intensive

task in DayMOPS processing. Unlike other stages, which consider only a night's-worth of data at a time, it must consider tracklets from many nights and find linkages between them. In order to build a useful track, suitable for orbit fitting, we need to link tracklets from three separate nights, within our sliding window of time (generally we use 15 days for this time window, to make the computations manageable). In general, this task scales exponentially with the number of tracklets, the time between observations, and the velocity limits for the tracklets. Thus it can quickly become overwhelming with dense source data, high velocity and acceleration limits, poor merging of tracklets, and long time windows.

To tackle this problem, we use an algorithm for performing this track discovery presented by Kubica et al. (Kubica (2005), Kubica et al. (2005)). In essence, the idea behind the algorithm is to build per-image 4D-Trees of (RA position, Dec position, RA velocity, Dec velocity), and use these to hold the tracklets, indexed by position/velocity. We then imagine the KD-Trees as hierarchical bounding boxes, and consider pairs of bounding boxes from different nights, calculating whether they could be linked by some acceleration factor less than our maximum acceleration threshold. If the boxes could be linked, then a track may exist within their contents and we continue searching bounding boxes lower in the tree hierarchy; if not, we know that no track of interest to us could pass through the boxes and we can abandon searching immediately. By using the hierarchical structure of the KD-Trees, we can avoid searching in large areas of tracklet-space where no track could ever exist, greatly reducing our workload. While these are similar to the KD-trees used in findTracklets, they are more complex because of the higher dimensionality (4D instead of 2D) and there are many more trees involved (each individual image is represented by a tree instead of one tree for an entire night's data, as in findTracklets).

2.4.1. Recursive Tree-walk Using Pruning

In the linkTracklets algorithm, all tracklets starting in a given image are placed in a single 4D-Tree containing bounding boxes in (RA position, Dec position, RA velocity, Dec velocity)-space. One tree is created for each of the images. It is then possible to calculate the acceleration needed for an object in one bounding box in one tree to reach (*i.e.* be compatible with) the second bounding box in a later tree. Because we are generally interested in tracks which have acceleration within a fixed range (e.g. between $> .02 deg/day^2$ and $< -.02 deg/day^2$), we can abandon searching at a given pair of bounding boxes if the necessary acceleration is outside our range of interest.

The minimum and maximum acceleration connecting two bounding boxes is currently calculated as follows:

$$maxAcc = \min \left(\begin{array}{c} \dfrac{Node2.maxV - Node1.minV}{dt} \\[2mm] \dfrac{2}{dt^2}\left(Node2.maxP_0 - Node1.minP_0 - Node1.minV \times dt\right) \\[2mm] \dfrac{2}{dt^2}\left(Node1.maxP_0 - Node2.minP_0 + Node2.maxV \times dt\right) \end{array} \right) \qquad (1)$$

$$minAcc = \max \left(\begin{array}{c} \dfrac{Node2.minV - Node1.maxV}{dt}, \\[2mm] \dfrac{2}{dt^2}\left(Node2.minP_0 - Node1.maxP_0 - Node1.maxV \times dt\right), \\[2mm] \dfrac{2}{dt^2}\left(Node1.minP_0 - Node2.maxP_0 + Node2.minV \times dt\right) \end{array} \right) \qquad (2)$$

Issue: Note that this approach simplifies the problem by treating the sky as a flat plane, which will be problematic near the poles. However, the above calculation appears to be the "hot spot" of the linkTracklets algorithm and accounts for most of the computation time, and so simplifying to reduce floating point costs greatly improves performance.

In the code, this calculation is performed by the function `updateAccBoundsReturnValidity` in `linkTracklets.cc`.

Pruning allows the rapid avoidance of searching in areas where no track can exist. As a simplified introduction to the full algorithm, see Figure 9 for a two-tracklet-linking, "endpoint-only" version of the algorithm which finds pairs of compatible tracklets on different nights.

Support Tracklets, Support Nodes, and the Full LinkTracklets Algorithm For orbit determination, we require detections on at least three separate nights. The endpoint-only algorithm in 9 will only attempt to find pairs of tracklets, giving tracks with only two nights of observational data. In practice, we seek to find tracks with tracklets from three unique nights. This could be accomplished using various extensions to the endpoint-only algorithm, but it is argued in Kubica (2005) and Kubica et al. (2005) that by far the most efficient of these variants is called the algorithm called the **vtrees** (for "variable trees") algorithm.

In the vtrees algorithm, we search for tracks with one or more intermediate "support" tracklets in between the "endpoint" or "model" tracklets (the first and last tracklet). To

accomplish this, the vtrees algorithm searches for compatible endpoint nodes as in Figure 9 but, as search progresses, maintains a list of compatible "support" nodes - nodes which could hold useful intermediate tracklets between the tracklets in the endpoint nodes. These are filtered at each step, again using the equations 1 and 2. As the search descends through the possible valid combinations of endpoint nodes, the support list is filtered and refined. When search terminates at a pair of leaf nodes, the support nodes are used to find possible support tracklets. If the support list ever becomes empty, we can prune the searching at this point, since we know no useful track (no track with at least three nights of data) could exist between the endpoint nodes.

The full vtrees algorithm is presented in Figure 10. This is the actual algorithm implemented by the function `doLinkingRecurse` from `linkTracklets.cc`

In the algorithm, support nodes are filtered and possibly split (and their children filtered) at each recursive step. Choosing when to split the support nodes is an important performance question. If we split too aggressively, then we will add more items to S and be required to filter a larger number of nodes at each recursion, which will increase cost at each step. If we split support nodes too rarely, then the support nodes may become very large relative to the endpoint nodes and we will often find that we have some compatible support node, and thus continue searching - even in cases where, had we split the support nodes, we would have seen that none of the leaf nodes held by the larger box were consistent with our position/velocity/acceleration range. This leads to needless searching when we should have simply terminated.

Currently, the cutoff for splitting is based on the spatial size of the support node relative to that of the two endpoint nodes. First a weighting factor, α, is calculated:

$$\alpha = \frac{supportNode.time - nodeA.time}{supportNode.time - nodeB.time} \tag{3}$$

We then split the node if, for *any* of the spatial axes (RA position, Dec position, RA velocity, or Dec velocity):

$$\left(\frac{width(nodeA.axis)}{\alpha} + \alpha \times width(nodeB.axis) \right) < 4 \times width(supportNode.axis) \tag{4}$$

Where *width* is the spatial extent of the node. This approach was developed by Jeremy Kubica through empirical testing, and may or may not be optimal for our data; however, in our experience, it seems to be effective.

The splitting and filtering of the support trees is implemented by `splitSupportRecursively` in `linkTracklets.cc`. This function uses several helper functions, including the same `updateAccBoundsReturnValidity` function used to check the compatibility of endpoint nodes.

2.4.2. Track Validation

Once a pair of endpoint tracklets and one or more support tracklets have been found via the vtrees algorithm, we may attempt to finally build a track from them. This is relatively straightforward; three or more tracklets with compatible acceleration, from three or more nights, have already been found. However, this acceleration factor is rather approximate, as it is based on the position and velocity estimate of the tracklets, not the best-fit to the detections held in the tracklet. Thus, at this point we actually start examining the detections themselves.

The track fitting is conducted in the method `calculateBestFitQuadratic` in `Track.cc`. First the Dec values of the observations are fit to either a quadratic or higher order (despite the name of the method) function, using the residuals of the fit compared to the differences between predicted and actual positions to control the order of the fit. Then the RA values of the observations are fit, with the added complication of including a topocentric correction if one could be determined from the tracklet and is appropriate for the fitting function. The order of the function in Dec and RA do not have to be the same.

In the event there are multiple possible support detections at one of these image times, the best-fitting detection is chosen.

After the fit is determined, the chi-squared probability of the RA and Dec fits is calculated for the 'chi-squared probability filter'. If an insufficient number of valid detections are found or the chi-squared probability of the RA or Dec fits is higher than the predetermined cutoff, the potential track is rejected. If it is validated, then it is passed to the set of output tracks.

2.4.3. Issues and Quirks

Topocentric Correction We can generate more precise fits and do more aggressive filtering if we first apply a topocentric correction to the detections, converting from topocentric coordinates to geocentric coordinates based on an assumed topocentric distance. For this reason, before the positions/velocities of the tracklets are calculated, the trees are built or

the linking algorithm is run, topocentric correction factor is calculated for each tracklet. This factor is then applied to the RA value of each detection in the tracklet when the track is being evaluated for residuals between the best-fit path across the sky (in RA/Dec) vs the locations of the actual detections. The correction is only applied in RA rather than Declination; the effect is small in declination.

Issue: I would like to see this verified across the entire sky, as it was developed near the equator/ecliptic.

Spherical Geometry Issues   Currently, the tracklet tree constructor in `TrackletTree.cc` will alter RA (and if needed, Dec) values so that all RA (and possibly Dec) values are stored on a contiguous 180-degree region. This simplifies the critical "hot-spot" calculations in `updateAccBoundsReturnValidity`, since we do not need to check for values which cross over the 0/360 line in RA. However, this means that if the input data covers too large an area of the sky then the acceleration range calculation will likely fail, and thus the whole algorithm will misbehave.

Further, as mentioned in section 2.4.1, we simplify the math throughout track generation by treating the sky as a flat plane, which will lead to significant distortion near the poles. This problem is often addressed by rotating the data in question so that it is centered on the RA, Dec origin (0,0), where polar distortions are minimal. This could be done for the entire input set of detections, but if the detections cover a sufficiently large area of the sky then we will not significantly reduce the problem. Temporarily re-centering the relevant points at each call to `updateAccBoundsReturnValidity` would likely work, but would probably be quite expensive. This is a problem which needs to be addressed eventually, perhaps by changing the equations used in 2.4.1, or per by rotating the bounding boxes per-query, so that the endpoint images will always be roughly centered over the origin.

Issue: Due to manpower constraints, we have not been able to test how big a problem this is, if the acceleration calculations are failing, and to what degree assuming the sky is 'flat' is distorting acceleration and compatibility calculations. It might be interesting to look at placing these trees into a x/y/z/vx/vy/vz sphere instead of the current RA/Dec/vRA/vDec coordinates. It is worth remembering that most of our tests have been using 15 day windows, so over most of the sky we will not have detections that cover much more than 180 degrees in RA except potentially near the poles.

Special Considerations of KD-Tree Construction for linkTracklets   Astrometric error on detections will affect both the position and velocities of true tracklets. As a result,

bounding boxes must be extended to encompass not just the tracklets which they hold, but the surrounding error bars. Each tracklet will have a unique error bar on its velocity, as tracklets will span different distances in RA and Dec (dp) and may also span different numbers of images and thus have different dt:

$$minV = (dp - 2 \times astrom\_err)/dt \tag{5}$$
$$maxV = (dp + 2 \times astrom\_err/dt \tag{6}$$

Thus, each node in the tracklet KD-Tree will have its position range extended by:

$$minP_0 = P_0 - astrom\_err \tag{7}$$
$$maxP_0 = P_0 + astrom\_err \tag{8}$$

and its velocity range will be extended to encompass the $minV$ and $maxV$ of all its child tracklets. These rules apply to leaf nodes as well as non-leaf nodes, which must have bounds at least as great as their child nodes. Note that as a result of expanding the boxes around tracklets, KD-Tree nodes may actually overlap.

Note that for linkTracklets, a leaf node's bounds should only extend as far as the error bars around their tracklets, and the non-leaf nodes should encompass only the area around their children's bounds. One of our early implementations did not follow this rule, and instead partitioned the space in a "top-down" fashion as in the left side of Figure 11, and it then handled the issue of error bars in the acceleration calculation function. This was technically correct, but lead to horrific performance - 1,000 or 10,000 times slower than the current version, illustrated on the right side of Figure 11. This is because the earlier version had nodes which encompassed larger areas of tracklet-space and thus sets of nodes were more likely to appear compatible, which results in less search pruning.

The former type of tree is simpler to construct (and perhaps easier to visualize when debugging). This is the type of tree used in most the other algorithms, which perform range searches and thus can extend handle their error bars per-query by extending their ranges as needed. However, the latter type of tree is the one needed for linkTracklets, and is implemented by the KD-Tree subclass `TrackletTree` in `TrackletTree.cc`.

Performance Enhancements for Acceleration Range Calculation As noted earlier, the function `updateAccBoundsReturnValidity`, which implements the equations 1 and 2,

accounts for most of the CPU time spent in linkTracklets. Thus, optimizing performance in this section of code is critical.

Rather than evaluate all arguments to min and max functions at the outset, the code attempts to evaluate each possible argument. If it becomes clear at any point that $minAcc > maxAcc$, then we know that the search can be pruned and the function returns immediately.

As an additional optimization, we start with $minAcc$ and $maxAcc$ set to the values used by our caller in the recursive searching. We know that the caller was examining two endpoint nodes which were either equal to or a parent of our current nodes, and thus our parents $(minAcc, maxAcc)$ range will be greater than the one we calculate. (For the initial start of the recursion, we use the user-specified min/max acceleration thresholds, because we do not care about any values outside this range anyway.) By doing this, we actually have a $maxAcc$ value available as soon as we calculate our first possible $minAcc$ value and vice-versa; this allows the earliest possible termination. However, it does make the code somewhat more confusing to read.

This confusion is somewhat amplified by the fact that this same `updateAccBoundsReturnValidity` function is used for filtering support nodes. In this case, the initial $minAcc$ and $maxAcc$ values are taken from the acceleration range calculated when examining the endpoint nodes $nodeA$ and $nodeB$, since we are not interested in finding acceleration values which connect $nodeA$ and a support node unless they also connect the support node to $nodeB$.

This is not an issue, just an explanation of the reasoning for including $minAcc$ and $maxAcc$ values from the parent and endpoint nodes.

2.5. Subset Removal

Some tracks are **subset tracks** of other tracks; that is, occasionally detections linked by one track found by linkTracklets will be a subset of those linked by another track in the same output set. This can arise for a variety of reasons, but occurs most commonly when a real object generates tracklets on four or more nights within a linking period. We generally expect that these subset tracks are unhelpful, and because they increase the size of the set of tracks sent to orbit determination, they are possibly costly.

Finding and removing subset tracks could be accomplished with a very naive double-for loop over the set of tracks, but of course this does not scale to larger data sets ($O(n^2)$ for n tracks). A more efficient algorithm uses a detection-to-track "reverse-map" R, which maps from each detection to the set of tracks holding that detection. This is easy to construct for

a set of tracks T:

---

   for $t_i \in T$ **do**
       $R[d_j] = \{\}$
   end for
   for $d_j \in t_i$ **do**
5:     $R[d_j] = R[d_j] \cup t_i$
   end for

We may then use the algorithm from Figure 12, which makes use of this reverse-map. The underlying idea is this: for each track t_i, we seek to find any track containing all the detections in t_i; any track containing all these detections must be equal to or a superset of t_i.

Subset tracklets can also occur when collapseTracklets is used. The same algorithm and software can be used to remove subset tracklets from a set of tracklets as well.

The reverse-map is implemented with a C++ `std::map`, allowing logarithmic-time lookups, and its contents are C++ `std::set`s, which allowing linear-time intersection calculations. However, both structures are implemented with trees; between the tracks themselves and these tree structures, this algorithm can require significant amounts of memory, and no distributed-memory equivalent is currently known to us. Fortunately, we have had good luck with distributed shared-memory approaches for large data sets (this is documented somewhere by Jon Myers in work with SDSC Dash; however, in practice with the improved filters on the linkTracklets output the large memory requirement is reduced and we could just run orbit fitting on everything).

2.6. Notes on Software Development

2.6.1. Accomodations for Large Data Sets

Over the course of our experiments, we discovered that under some circumstances, tools may return some very large data sets - larger than the memory available on our development machines. Though RAM sizes may grow over time, it is likely that dayMOPS users will continue to experiment with increasingly dense noise or loose limits, resulting in increasingly large numbers of tracklets or tracks.

To help deal with this problem, the `findTracklets` and `linkTracklets` functions can be configured to output their results in various ways; they can be configured either to store their results in memory and return them (much like a normal function call) or to return nothing and write results directly to file. If the user is confident that the data set to be returned will fit in memory, the former is more elegant (and fits better with the LSST model of passing data to and from worker nodes through memory only), but for our experiments we always write to file, in case the number of tracklets or tracks discovered is large.

The `findTracklets` and `linkTracklets` functions each take as an argument an object of type `findTrackletsConfig` or `linkTrackletsConfig`; each type has a public member variable called `outputMethod` which can be set. `findTracklets.h` and `linkTracklets.h` each contain enum types which can be used to set these flags.

Dealing with larger-than-memory data sets as input to our software tools is a more significant problem. We generally assume that the number of input detections will fit in memory, and that KD-Trees of these detections will also fit in memory. This has always been the case, and fortunately it is easy to predict whether a set of detections will fit in memory or not. However, the number of tracklets or tracks may, depending on the data and configuration of the software, grow to be quite large, and is not trivially predictable. For software which uses tracklets or tracks as its input data and operates on them in bulk (including `collapseTracklets`, `removeSubsets`, and `linkTracklets`), this may be problematic.

2.6.2. Parallelization

We have parallelized the various linking stages of DayMOPS using multithreading, implemented using OpenMP (see the code versions ending with OMP in the repository). This allows multiple CPU cores to work simultaneously on the data set, but does not address the problem of partitioning the data sets between machines. This means that multithreading can be effective in large-memory environments, but does not attempt to solve the problem of larger-than-memory data sets.

The issue of larger-than-memory data sets could be addressed in several ways: through (OS-level or implementation-level) distributed shared memory, algorithmic changes, or simply requiring large-memory machines. We have explored using kernel-level distributed shared memory provided by the vSMP software on the Gordon cluster at San Diego Supercomputing Center. This software runs inside the OS kernels of various machines connected via network, and provides the appearance that all CPUs and RAM on the various machines are shared on a single motherboard. A similar effect could be achieved through explicit use of a user-

level distributed shared memory library (such as memcached), but would require additional coding.

Parallel FindTracklets

In our current version, we parallelize the work being done per-detection. This is achieved with a simple **parallel for** loop replacing the **for** loop at line 12 in the pseudocode at Figure 6. Because the amount of work done will vary per-detection, depending on how many possible second endpoints are found, we use dynamic thread scheduling as opposed to static scheduling. The only critical section used is the writing of results, otherwise there is no need for inter-processor synchronization or communication.

The tracklets reported by parallel findTracklets should be identical to those reported by serial findTracklets, though the order in which they are reported may differ.

Parallel CollapseTracklets

The work done is parallelized on a per-tracklet basis. Again, this is achieved with a simple **parallel for** loop replacing the **for** loop at line 8 of Figure 7. The writing of output is inside a critical section, as in parallel findTracklets.

Unlike findTracklets, the work done in the parallel region of collapseTracklets is not entirely independent; different threads may read and write the "already merged" flags on tracklets. This leads to a potential consistency problem, with several possible solutions. One approach would be to enforce strict locking on every read/write to the "already merged" flags. This has the disadvantage of potentially scaling very badly, since the reads/writes are extremely frequent and synchronization costs could be quite high. It is also problematic in that it creates potential for deadlocks if not implemented very carefully. A second approach would be to disregard the flags entirely, which would be quite simple to implement. However, in cases where objects may generate many tracklets (e.g. deep stacks, which can see n^2 tracklets given n observations) this would result in a significant amount of redundant work being performed. We took a third approach, which attempts to compromise between these two: we do not enforce strict locking on the "already merged" flags, and simply allow that there may be stale reads occasionally. These stale reads may lead to redundant work, but because we expect that they will be uncommon in general (perhaps not in deep stacks), this should not have too big an impact on performance. The redundant work will lead to redundant tracklets in output, but we expect them to be removed by the removeSubsets stage.

It is also important to note that because of the "already merged" flags, results from collapseTracklets are nondeterministic in a multi-threaded environment. Consider the unusual case in which tracklets t_a and t_b are sufficiently close in the tree, and t_b and t_c are sufficiently close in the tree, but t_a and t_c are not sufficiently close in the tree, and querying for one will not return the other. Depending on which tracklet is first visited and queried for similar tracklets, tracklet t_b may be merged with either t_a or t_c, at which point it will be flagged and never considered again. As a result, output from parallel collapseTracklets runs is expected to vary, and not just with regard to ordering, albeit quite slightly.

Parallel LinkTracklets

LinkTracklets looks for tracks which could start in a given image and end in another given image. Usually, the number of possible start/endpoint image pairs is fairly large, so this provides a natural axis of paralellism. The psuedocode for the parallel linkTracklets is presented in Fig. 13.

Unlike the other parallel programs, which write their output inside of a critical section, parallel linkTracklets maintains separate output sets for each thread, so it has no critical sections at all. This allows for slightly better scaling of performance. The parallel linkTracklets should return the same tracks discovered by the sequential version, though the order of their discovery may differ.

Parallel Subset Removal

Again, the subset removal algorithm contains an outer **for** loop which provides an obvious axis of parallelism. The **for** loop at line 8 of Figure 12 is simply changed to a parallel **for** loop to achieve multi-threading parallelism.

The work done in the parallel section is natrually independent, so the only critical section is the writing of output. The results of parallel subset removal should be identical to that of the sequential version, except for the ordering.

Require: I is a set of images, each of which has an associated exposure time and contains a set of detections

          ▷ Create a 2D KD-Tree for each image, holding detections from that image.

    $T \leftarrow \emptyset$

    for $i \in I$ **do**

        $t \leftarrow \text{Make2DTree}(i.detections)$

5:      $t.time \leftarrow i.time$

        $T \leftarrow T \cup \{t\}$

    end for

                             ▷ Use these trees to discover the actual tracklets.

    $tracklets \leftarrow \emptyset$

10: **for** $t_1 \in T$ **do**

        $later \leftarrow \{t_i \in T : 0 < t_i.time - t_1.time < maxDt\}$

        for $d \in t_1.detections$ **do**

            for $t_q \in later$ **do**

                ▷ Use time between images and max velocity to calculate the max travel distance

15:             $dt \leftarrow t_q.time - t_1.time$

                $dd \leftarrow dt * maxV$

                  ▷ Use KD-Tree range search to find detections within max travel distance

                $tracklets \leftarrow tracklets \cup t_q.\text{rangeSearch}(d.ra, d.dec, dd)$

            end for

20:     **end for**

    end forreturn $tracklets$

Fig. 6.—: Pseudo-code for the findTracklets algorithm. 2D (RA, Dec) trees are created for each image; for each detection, later trees are searched for nearby detections.

Require: T is a set of intra-nightly tracklets, D is the set of nightly detections from which T was created, *range* is a 4-tuple of tolerances for RA, Dec, angle and velocity.

 $t_c \leftarrow midpoint(\{d_{time} : d \in D\})$

 for $t \in T$ **do**

  Calculate t's predicted location at time t_c, its motion angle and velocity

 end for

5:   $\triangleright$ Create a 4D KD-Tree of the tracklets on their projected RA, Dec position and motion angle/velocity.

 $tree \leftarrow \text{Make4DTree}(T)$

 $outTracklets = \emptyset$

 for $t \in T$, t has not already merged with another tracklet **do**

     $\triangleright$ Find tracklets with projected location, motion similar to that of t

10: $candidates \leftarrow tree.\text{rangeSearch}(t_{projected\ position}, t_{angle}, t_{velocity}, range)$

  for $c \in candidates$ **do**

   if c and t do not contain different detections from the same image **then**

    $t.detections \leftarrow t.detections \cup c.detections$

    mark c as already merged

15:   **end if**

  end for

  mark t as already merged

  $outTracklets \leftarrow outTracklets \cup t$

 end forreturn $outTracklets$

Fig. 7.—: Pseudo-code for the collapseTracklets algorithm. A 4-D KD-Tree over RA, Dec, angle, velocity is constructed using the projected locations and motion of the tracklets. Tracklets which are similar in this 4-D space are roughly colinear, so they are merged and written to output.

Require: T is a set of tracklets, $rmsMax$ is a maximum root-mean squared residual on the
tracklet's best-fit function to its detections

    for $t \in T$ **do**

        $rms = RMS(t)$

        while $rms > maxRms, |t| > 2$ **do**

            remove the worst-fitting detection from t

5:          $rms = RMS(t)$

        end while

    end forreturn $outTracklets$

Fig. 8.—: In purifyTracklets, poorly-fitted detections are "pruned" from tracklets. In certain degenerate cases, we may prune tracklets down to only two detections, in which case the two-detection tracklet is kept.

Require: $nodeA$ and $nodeB$ are KD-Tree nodes which hold tracklets from two different images on different nights, $minAcc$ and $maxAcc$ specify the limits of accelerations which the user finds interesting.

    $accRange$ = min/max acceleration to move from $nodeA$ to $nodeB$

    if $accRange$ does not overlap $(minAcc, maxAcc)$ **then return** $\emptyset$

    else

        if $nodeA$ and $nodeB$ are leaf nodes **then**

5:                $\triangleright$ When we hit a pair of terminal nodes, and their acceleration bounds are interesting, then we have found a set of tracklets which may be sufficient to create a track.

           return {tryToBuildATrack($nodeA$.tracklet, $nodeB$.tracklet)}

        else

                $\triangleright$ In order to ensure that this function sees nodes which are roughly the same size, we choose the larger node and "split" that one, recursing on its children.

           $largerNode, smallerNode \leftarrow orderBySize(nodeA, nodeB)$

           $leftRes \leftarrow recurse(largerNode$.leftChild$, smallerNode, S)$

10:           $rightRes \leftarrow recurse(largerNode$.rightChild$, smallerNode, S)$ **return** $leftRes \cup rightRes$

        end if

    end if

Fig. 9.—: An endpoint-matching, two-tracklet version of the linkTracklets algorithm. Note that if two nodes have no chance at holding a compatible tracklet (first "if" check) then their children are never searched; only if they may hold an interesting track are the children searched. In this way, the algorithm avoids even examining a great number of KD-Tree node pairs and thus the pairs tracklets contained therein.

Require: $nodeA$ and $nodeB$ are KD-Tree nodes which hold tracklets from two different
images on different nights, S holds a series of nodes from images take on nights in between
$nodeA.time$ and $nodeB.time$, $minAcc$ and $maxAcc$ specify the limits of accelerations
which the user finds interesting.

$accRange$ = min/max acceleration to move from $nodeA$ to $nodeB$

if $accRange$ does not overlap $(minAcc, maxAcc)$ **then return** $\emptyset$

else

    for $supportNode \in S$ **do**

5:        **if** $supportNode$ represents an awkwardly large portion of tracklet-space relative
to $nodeA$ and $nodeB$ **then**

            replace $supportNode$ with $supportNode.rightChild$ and
$supportNode.leftChild$, coming back to them later

        else

            if no track with acceleration within $accRange$ could pass from $nodeA$ through
$supportNode$ and into $nodeB$ **then**

                remove $supportNode$ from S

10:            **end if**

        end if

        if S is empty **then return** $\emptyset$ ▷ There is no way to build a three-tracklet track
using the contents of these nodes, so abandon searching.

        end if

    end for

15:    **if** $nodeA$ and $nodeB$ are leaf nodes **then**

                ▷ Again, try to build a track, this time using S for intermediate tracklets

     return $\{$tryToBuildATrack($nodeA$.tracklet, $nodeB$.tracklet, S)$\}$

    else

        $largerNode, smallerNode \leftarrow orderBySize(nodeA, nodeB)$

        $leftRes \leftarrow recurse(largerNode.\text{leftChild}, smallerNode, S)$

20:       $rightRes \leftarrow recurse(largerNode.\text{rightChild}, smallerNode, S)$ **return** $leftRes \cup$
$rightRes$

    end if

end if

Fig. 10.—: The full vtrees algorithm, the actual algorithm implemented in linkTracklets.
At each recursion, S, the set of support nodes, is split based on the position, velocity, and
acceleration range implied by the $nodeA$ and $nodeB$, the two endpoint nodes. Note that
if support nodes are periodically "split" and replaced with their chidlren if they too large
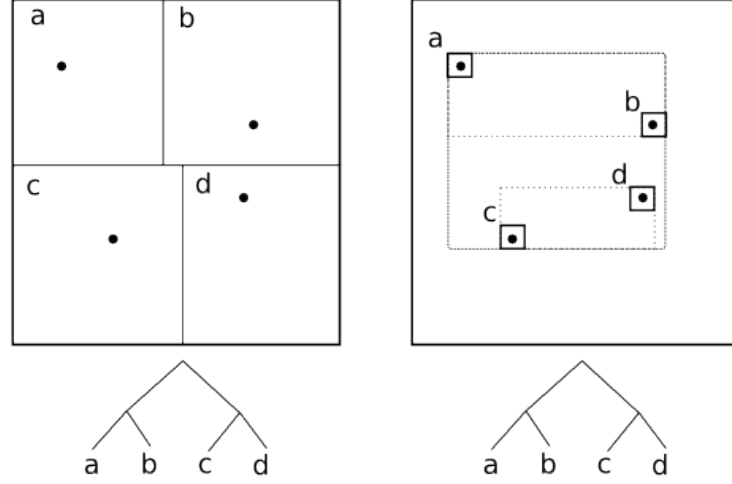relative to $nodeA$ and $nodeB$.

Fig. 11.—: Two possible ways of constructing a KD-Tree over four points. The left shows a top-down tree; the right shows a tree constructed from the bottom up and with non-leaf branches extending only as far as their children's bounds.

---

for $t_i \in T$ **do**
    candidates $= T$
    for $d_j \in t_i$ **do**
        candidates $=$ candidates $\cap\ R[d_j]$
5:    **end for**
    if $|\text{candidates}| > 1$ **then**
        t_i is a subset of some other $t_j \in T$; discard it
    else
        keep t_i
10:   **end if**
end for

Fig. 12.—: Psuedocode for the subset removal algorithm

Require: T is a set of per-image tracklet trees

$work \leftarrow \emptyset$

for $t_i \in T$ **do**

    for $t_j \in T$ and t_j happens ≥ 2 nights later than t_i **do**

        if there are sufficient support trees between t_i and t_j **then**

5:           add t_i, t_j to work

        end if

    end for

end for

parfor $w \in$ work **do**

10:    $t_i, t_j \leftarrow w$

    $sup \leftarrow$ trees from images between t_i and t_j

    use vtrees algorithm (Fig. 10) to find tracks starting in t_i, ending in t_j and passing through sup

end parfor

Fig. 13.—: Psuedocode for parallel linkTracklets. First, usable pairs of images are identified in a single thread, then the searching between these pairs of images is performed in parallel by multiple threads.

3.   Metrics & Scaling of DayMOPS linking algorithms

Current development efforts have focused on the linking phase of dayMOPS, as all later processing is dependant on its success. Existing orbit determination packages claim a high rate of success for accurate Orbit Determination (OD) given a correctly-linked track, and should correctly reject false tracks in nearly all cases (Milani et al. 2006). As a result, we expect that the ability of the system to successfully discover solar system objects in the data given to dayMOPS will be determined primarily by the linking component and its ability to send useful tracks to OD. We also expect the overall resource usage of the dayMOPS system will be calculable given the runtime of the sky-plane tracking component, the number of tracks it passes to OD, and the per-track OD time of our OD package. As a result, carefully studying the behavior and output of the sky-plane linking should provide a reasonable estimate of the resource usage of all of dayMOPS object discovery.

3.1.   Metrics for End-to-end Evaluation of Sky-plane Linking

Because the number and density of input diaSources, as well as the cadence of observations, are important parameters for evaluating the performance of dayMOPS, we have generally chosen to test on simulated data. In particular, this data simulates what LSST might pass to dayMOPS in diaSource catalogs, simulated directly from catalogs. As the rest of the LSST DM software improves, we will move to testing on diaSource catalogs resulting from simulated images from ImSim (thus containing more appropriate noise backgrounds and artifacts), but this data is not yet available. It would also be useful to test on real data, however data sets with the appropriate density of solar system objects (related to the depth of the images) and cadence are hard to acquire. By testing on simulated data, we have the advantage that we have a 'cheat' – we know the true identity of each diaSource and whether we are detecting a true or false track.

Because of our limitations with orbit determination at present, and because we are focusing on the linking stage of dayMOPS, we established the following set of conditions:

- A moving object is **found** if a track is generated by linkTracklets that consists only of detections from the moving object and consists of 6 different observations from at least three different nights. This should be enough information for orbit determination to generate a useful orbit, so practically speaking is a useful condition for considering an object 'found'.

- A moving object is **findable** if the number of observations of the object meet these

same guidelines: at least 2 observations within our tracklet time window (90 minutes) on at least 3 separate nights within the track time window (15 days), and velocity and acceleration limits below the chosen threshholds. Not all moving objects are observed by the telescope with the appropriate cadence, and not all objects fit within our current velocity and acceleration bounds.

When running simulations, determining whether or not a given object is findable is fairly straightforward, and determining which objects are found simply involves examining the output tracks.

Then, to understand the success and net cost of our linking, we can compare the objects found together with the compute cost for finding these objects. When measuring and optimizing the internal behavior of the dayMOPS system, it is helpful to study the quality and quantity of the intermediate data structures used (*i.e.* the tracklets, the number of findable objects compared to found, and the number of false tracks) as well.

The total number of tracks or tracklets is of significant concern when estimating the resource usage of the system. The number of tracklets will be a major factor in the predicting the workload of track generation, and the number of tracks should entirely decide the size of the workload for OD. As such, we measure the **number of tracks** and **number of tracklets**.

Correctly-linked tracks and tracklets are referred to as **true tracks** and **true tracklets**. We present the percentage of tracklets and tracks which are true in our results. Note that it is expected that multiple correctly-linked tracklets and/or tracks may be generated for a given found object, if the object is observed more than the minimum number of times as is the case in most of these simulations. Thus, we expect the number of true tracks and tracklets to significantly exceed the number of found objects, and the fraction of true tracks to findable objects can exceed 100%. Nonetheless, we find that checking the true/false ratio of tracklets and tracks helps to illustrate the quality of linkages used as input to the track generation software and to OD.

3.2.   Simulation test setup

To test MOPS, we generated one month of simulated asteroid detections, based on the image cadence of the Operations Simulator (run 3.61) between the dates 51029 and 51061. Pointings from around the full sky were used, but only pointings which were part of the Wide Fast Deep (aka 'universal') portion of the survey. Simulated asteroid detections were generated using the LSST Catalogs Simulation framework, by applying ephemeris generation to a

statistically viable solar system model containing 11 million objects (the Grav Solar System Model, SSM (Grav et al. 2011)). Objects which should have been detectable with a SNR of 5 or greater in a particular pointing were recorded into a detection catalog. Conservative per-image levels of astrometric error were added to the detection locations, depending on the SNR of the objects, the seeing in the image, and an assumed systematic astrometric error floor (about 0.2"). A plot showing the sky distribution of the detections used in the simulation is presented in Figure 14.
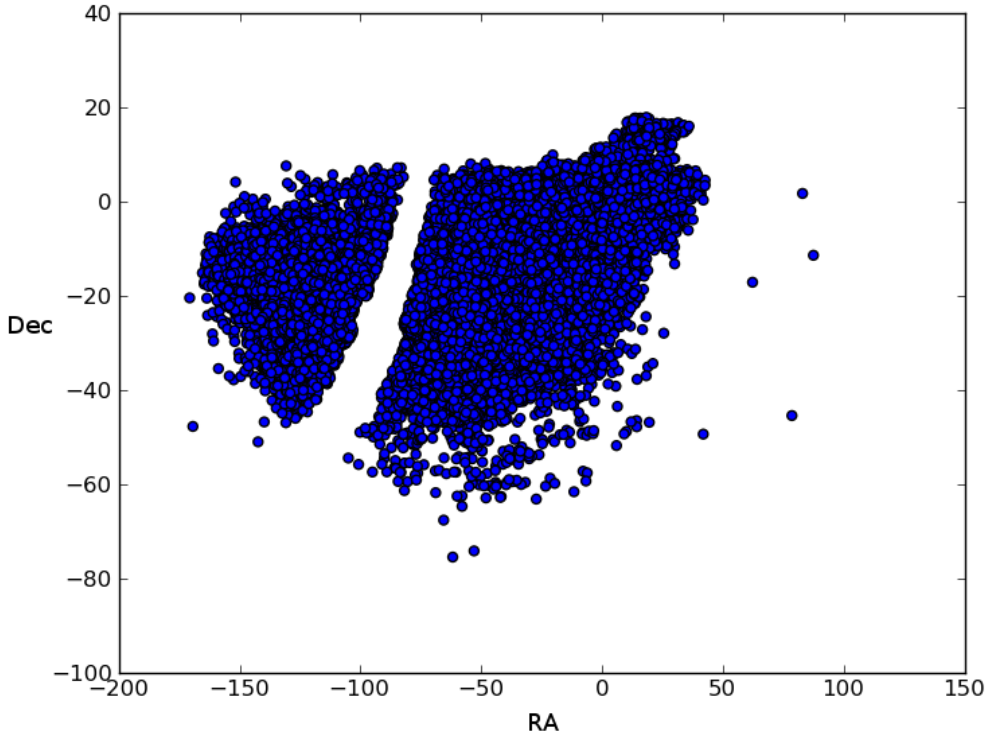

Fig. 14.—: A reduced-density plot of simulated asteroid detections (DiaSources) used in our simulated catalog.

3.2.1. Choosing the Linking Time-Window

As expected in production, we attempted to generate tracklets between any pair of images separated by more than 15 minutes and less than 90 minutes. However, for a more manageable track generation phase, we attempted to link tracklets if they were separated by ≤ 15 days; in production, it is expected that this number will be 30. These numbers should

be consistently true across all experiments presented here.

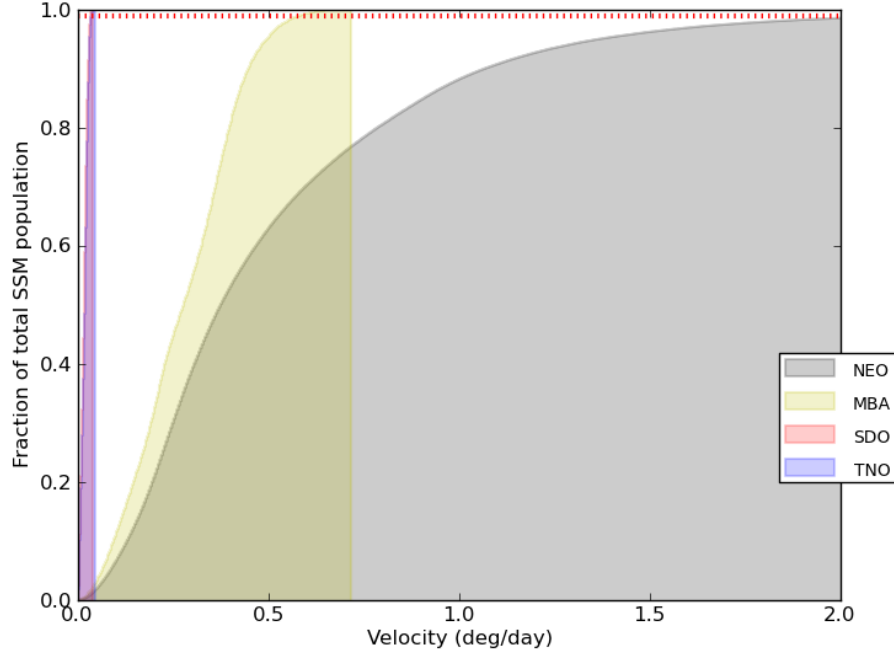### 3.2.2. Choosing Velocity and Acceleration Limits

Fig. 15.—: A cumulative histogram of solar solar system object sky-plane velocities, organized by classification. These velocities include objects at all solar elongations. Classes of objects closer to the Sun and to the Earth (NEOs) move faster than objects further away (TNOs).

We chose limits on velocity and acceleration by looking at the actual velocities and accelerations of objects from the SSM, after generating their ephemerides at a variety of times. Histograms of the velocities and acceleration distributions are shown in Figures 15 and 16.

As can be seen from these distributions, NEOs move fastest and with the highest accelerations, while outer solar system objects (SDOs, TNOs) move much more slowly. In order to detect 99% of all MBAs, velocity limits of 0.5 deg/day and an acceleration limit of .02 deg/day^2 are sufficient. It's worth noting that this is too slow to detect more than about 60% of the NEOs, but this is a simplifying choice made to make find and linkTracklets more manageable at this stage of development.
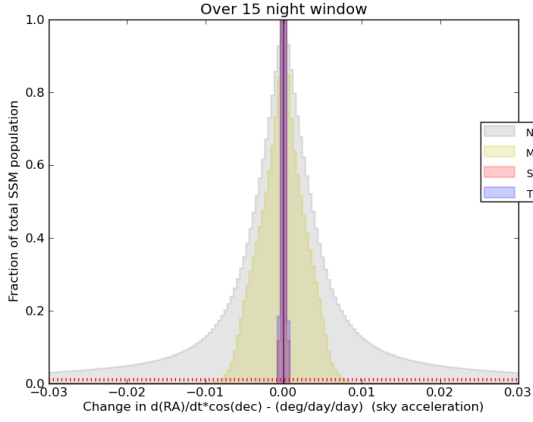
(a) Apparent Accelerations in Right Ascension over 15 Days
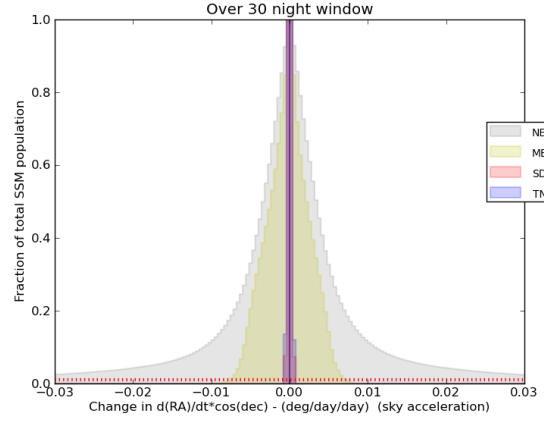
(b) Apparent Accelerations in Right Ascension over 30 Days
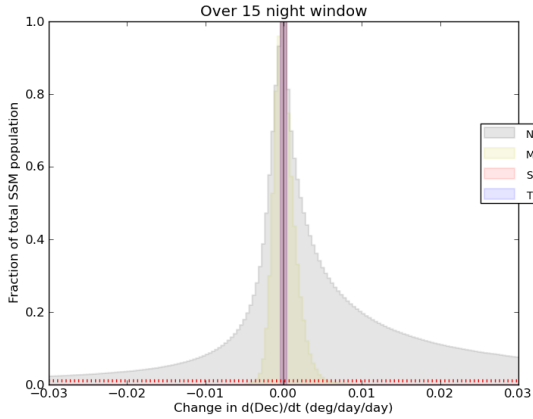
(c) Declination Apparent Accelerations in Declination over 15 Days

(d) Declination Apparent Accelerations in Declination over 30 Days

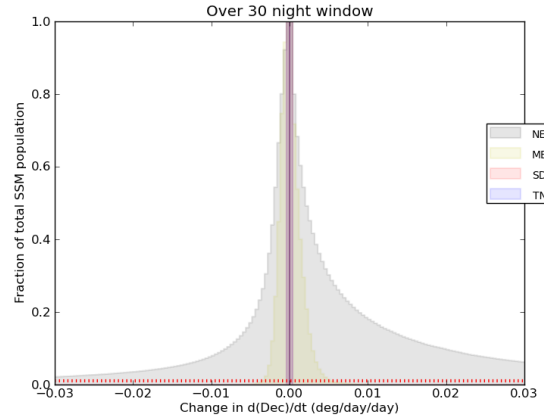Fig. 16.—: Normalized histograms of sky-plane accelerations of several classes solar system objects in the RA and declination, with objects grouped by classification. Histograms are presented for changes over 15 days and 30 days. The best-fit accelerations vary slightly given the size of the window; this is due to non-quadratic factors not included in the simple quadratic model. 15 day tracking windows are used in the experiments presented in this document, but we expect to move to 30 day windows in the future. In both cases, virtually all MBAs, and all other objects except NEOs, should have accelerations between -.02 and .02 deg/day^2 in both axes.

By examining the detections on an object-per-object basis, we calculated that among

the 186,344 objects seen with proper cadence, 186,209 of these (more than 99.9%) should generate useful tracks given these velocity and acceleration limits. This is a reflection of the fact that the overwhelming majority (about 9M of the total 11M) objects in the SSM are MBAs, while NEOs make up only a small fraction of solar system objects.

3.3. Simulation Results

All simulations were conducted on the Gordon cluster at San Diego Supercomputing Center. Because of the large memory requirements for running MOPS, the vSMP nodes were used for all stages of computation. Except for the scaling tests, 16 threads were used for all the runs.

Number of asteroid detections:	36,311,037
Number of non-asteroid detections:	0
Average detections per night:	1,134,719
Number of tracklets found:	12,890,181
Number of true tracklets:	6,859,331
Tracklets % true:	53.2%
Tracklet generation time:	4,791 sec (1.33 hours)
Tracklet generation memory use:	13.7 GB
Number of tracks found:	10,423,382
Number of true tracks:	5,779,424
Track % true:	55.4%
Track generation time:	36,237 sec (10.1 hours)
Track generation memory use:	16.2 GB
Number of found objects:	854,037
Number of findable objects:	1,128,643
Found / findable:	75.7%

Fig. 17.—: Results from the MOPS run without noise. Velocity limit was .5 deg/day, acceleration limit was .02 deg/day^2 and the track chi squared probability limit was .9. Note that not quite one fourth of objects which should generate plausible tracks are rejected.

3.3.1. Survey Efficiency

Figure 17 shows in-depth stats for a 'perfect' survey, where SSM detections above 5σ SNR in each image are reported without additional 'noise' from artifacts in difference imaging, background transient or variable objects, or cosmic rays. As in all our runs, track generation is far more expensive than tracklet generation in terms of CPU usage, but both require substantial amounts of memory. Also note that nearly one fourth of the findable objects (those which should generate useful tracks) are not found. While over time these objects may not be lost forever (*if* they are discoverable in other apparitions), this is a fairly dramatic inefficiency in discovery rate, especially when discovery losses due to survey cadence inefficiencies are considered. The cause of this inefficiency is not entirely clear at present, however there are indications it is linked to overly aggressive filtering in the chi-squared probability filter; examining the pre-determined cutoff, especially to see if the same cutoff should be applied over the entire sky, would be a first step.

Issue: This discovery rate of 75% is a significant issue for dayMOPS and should be investigated further. It's possible that simply tuning the chi-squared probability filter cutoff would fix the problem, although it could also be related to sky-plane distortion problems once the poles are included in the input data.

3.3.2. Nightly Variance in Runtime

The cost of running MOPS depends on a variety of factors which are largely dependent on telescope operations, such as revisit rates and the locations of revisits. If no fields are observed that could have compatible tracklets, then MOPS very quickly rules out these observations and so runtime is short; on the other hand, if having lots of potentially compatible detections means that runtime will be longer. Figure 18 shows the range of variations over the month of this simulation.

3.3.3. Scaling on Non-Asteroid Sources

Actual images will contain diaSources from non-asteroid sources: variable stars, supernova, and image processing artifacts (e.g. from bright stars) will also be present. Because the quality of image processing is not known, we added non-asteroid "noise" detections to images at varying rates. At each rate, a fixed n noise detections were added to each image, with locations chosen at random. This is not a truly realistic representation of the noise, as positions of actual noise sources could be highly correlated and thus mimic actual moving
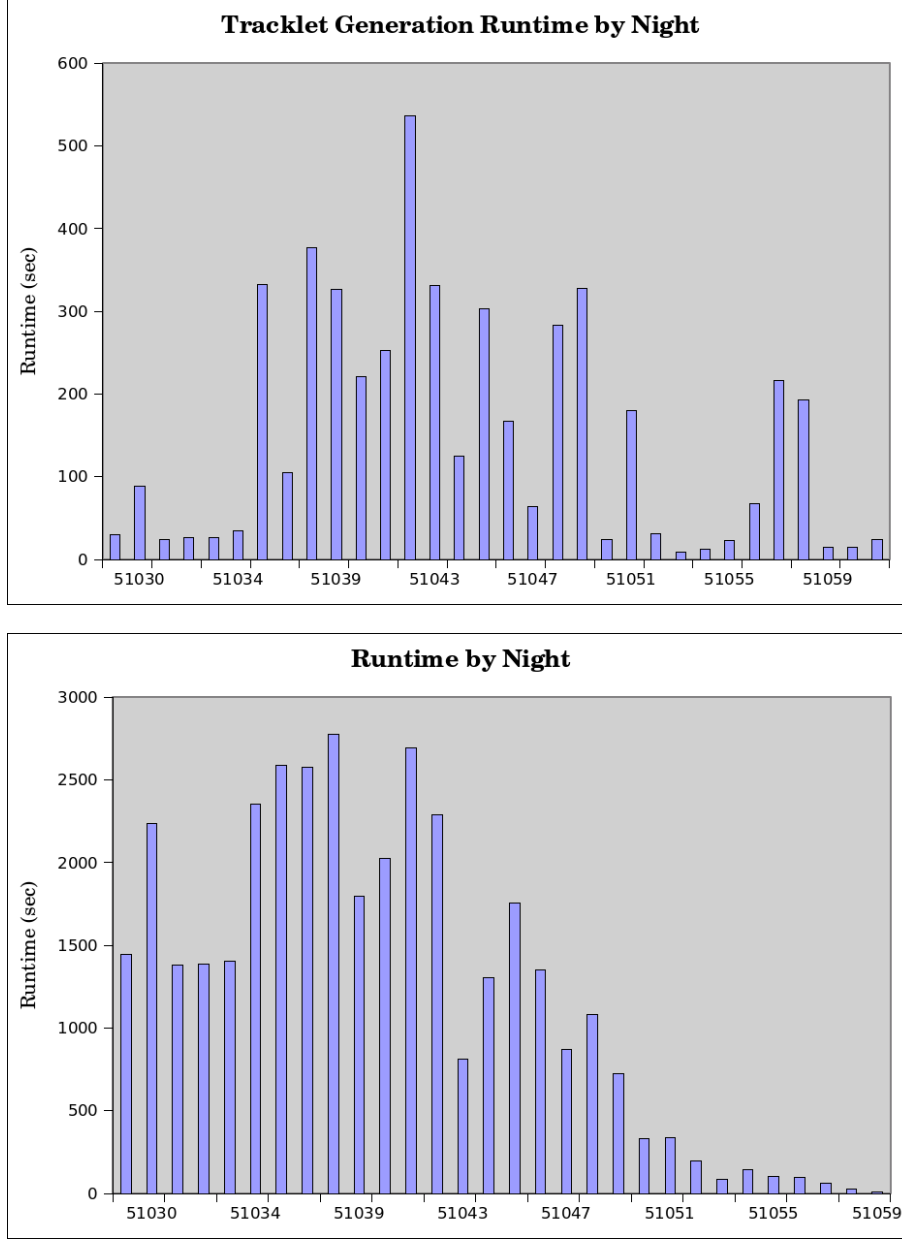
Fig. 18.—: Per-night costs of tracklet generation and track generation. Also, in the track generation section, note that because only 31 sets of nightly tracklets were generated, later runs had less data in their 15-day window and thus ran considerably faster. This is an artifact of the experiment and not a meaningful trend.

objects to preliminary stages of linking (thus making compute times increase). The response of dayMOPS to actual data may thus be quite different, but this was a reasonable starting point until more information is available.

We successfully ran the linking stages of dayMOPS using densities as high as 5,000 non-asteroid sources per image. After adding 10,000 non-asteroid sources per image, tracklet generation was possible but linking tracklets into tracks was too slow - at over 48 hours for a single night of searching, it exceeded the wall-clock limit on Gordon jobs.

Figure 19 presents a short summary of the input detection catalogs generated at each of the noise densities. For each of these catalogs, tracklet generation was performed for each of the 31 simulated nights of observation; results can be seen in Figure 20. As expected, increasing numbers of false detections lead to worse-than-linear increases in mislinkage. This lead to worse-than-linear increases in computational costs for generating the tracklets, both in terms of CPU and memory usage.

The tracklets generated in the tracklet generation test were used to test scaling of track generation. For reasons of time, we only attempted to search for tracks starting on the first night of observation (*i.e.* the first window of linkTracklets). Results are presented in Figure 21 and Figure 22. The CPU time cost for track generation scaled worse-than-linearly on the number of tracklets. However, we saw only modest increases in the number of output tracks and runtime for linkTracklets, meaning that we were able to successfully reject most of these false tracks during track validation. Also note that the number of objects found remained nearly constant across the various runs.

Per-Image Noise Density	Total number of detections	% noise detections
0	36,311,037	0%
1,250	72,258,537	49.7%
2,500	108,206,037	66.4%
5,000	180,101,037	79.8%

Fig. 19.—: An overview of the detection sets used for the scaling tests on noise density.

3.4. Conclusions

For LSST images, we expect that 50-80% of the DiaSources in our catalogs may be attributable to non-asteroid, real astronomical sources, before considering image subtraction artifacts. This corresponds to roughly 1250 or 5000 "noise" points per image, as we simulated.

To meet requirements, we must be capable of running one night's-worth of tracklet generation, track generation (using the entire previous 15 to 30 day window's worth of tracklets), and per-track IOD within 24 hours, plus precovery and attribution. For the 50% noise case, we saw a maximum tracklet generation time of 10 minutes (using 16 CPUs) and
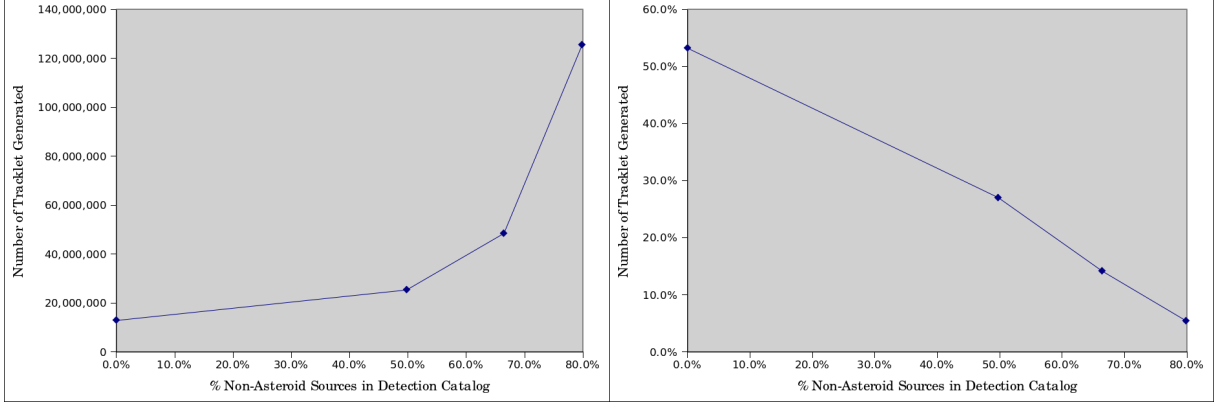
(a) Number of tracklets generated at various noise density levels

(b) Tracklet % true at various noise density levels
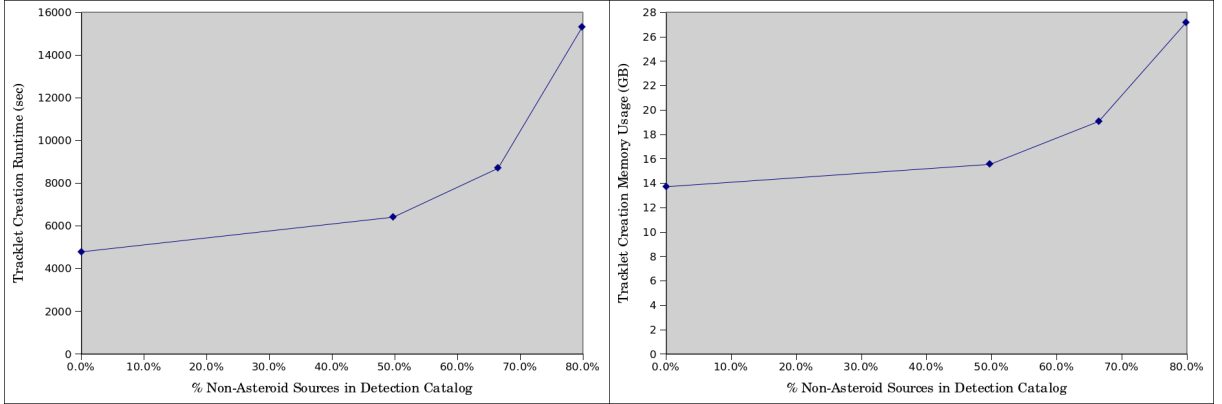
(c) Tracklet generation runtimes at various noise density levels

(d) Tracklet generation memory use at various noise density levels

Fig. 20.—: Tracklets generated at varying densities of non-asteroid "noise" sources, and corresponding compute costs. Each data point represents 31 days of tracklet generation. The same asteroid catalog was used for each simulation, but increasing numbers of "noise" sources were added in each simulation (see Figure 19). Note that the number of tracklets generated, and the computational costs to find them, increase quickly as noise density increases. This is apparently due to the increase of mislinked "false tracklets".

for the 80% noise case we saw a maximum tracklet generation time of 21 minutes (again using 16 CPUs). In our testing of track generation, we saw 306,866 tracks and 461,902 tracks generated in the 50%-noise and 80%-noise cases respectively. Expecting a trivially parallel IOD and an IOD cost of roughly .001 seconds/track, we anticipate that IOD should not be problematic: given a few hundred CPUs, we should be able to complete the nightly IOD processing in a few wall-clock hours.
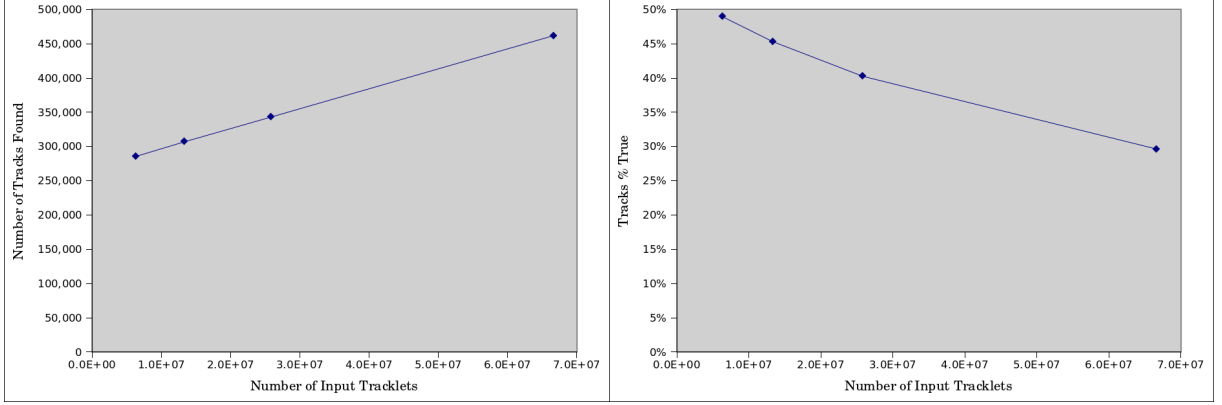
(a) Number of tracks generated at various noise density levels
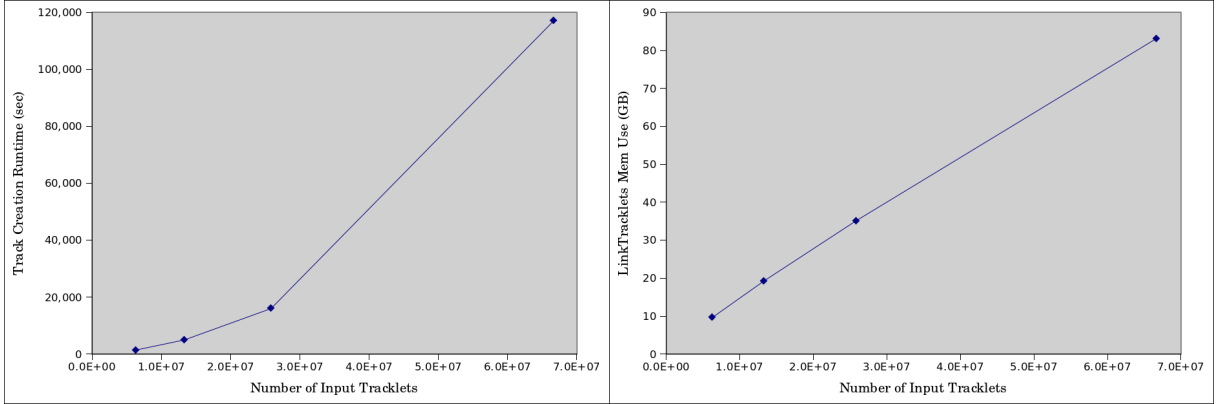
(b) Track % true at various noise density levels

(c) Track generation runtimes at various noise density levels

(d) Track generation memory use at various noise density levels

Fig. 21.—: Tracks generated at varying densities of non-asteroid "noise" sources, and corresponding compute costs. Detections catalogs with increasing numbers of noise detections (Figure 19) and tracklets generated from these catalogs (Figure 20) were used to generate linkTracklets input. For reasons of time, each linkTracklets run attempted to find only tracks which started on the first night of data and ended anywhere within the first 15 days.

The cost of running linkTracklets, however, could be problematic given the 24-hour limit. As seen in Figure 21 (c), linkTracklets can be quite slow, and runtimes can increase worse-than-linearly on the number of input tracklets, with non-linear factors becoming significant somewhere between the 50%-noise and 80%-noise cases. In the 50%-noise experiment, runtime for a single night was only 1.4 hours, but for the 80%-noise experiment, runtime was 32.5 hours! Again, both experiments used 16 CPUs.

Noise Density	Number of Tracklets	Found Objects
0	6,312,807	55,982
1,250	13,318,186	55,870
2,500	25,824,121	55,751
5,000	66,635,397	55,464

Fig. 22.—: Objects found by linkTracklets with varying densities of noise in the input catalogs. Note that the number of objects found is only slightly affected by the presence of noise in the input catalogs.

In our one-month run of linkTracklets without noise, we found the per-night cost of tracklet generation could vary by a factor of two or more (see Figure 18). Applying this to the runs performed with noise, this gives us an estimated maximum nightly runtime of between 2.8 and 65 hours (assuming 16 CPUs).

In order to reach the goal of running tracklet generation, track generation, and IOD on the tracks, we should aim to reduce the maximum runtime of linkTracklets to below 20 hours in the worst case. This requires a speedup of at least 3-4 over the current performance. Such a speedup may be possible simply by waiting on Moore's law, but it would be preferable to begin experimenting with larger numbers of threads and possible sequential optimizations as soon as possible, together with looking at potential improvements in the uderlying KD-Tree algorithms (such as optimizing the tree-walking code, making sure the leaf-node sizes are appropriate, checking support node splitting, and ensuring that memory is being accessed efficiently. It may also be worthwhile to explore GPUs in the context of parallelization, if trees can be efficiently split between different machines to reduce individual memory footprint requirements (such as was attempted with the preliminary work on a distributed linkTracklets algorithm by Matt Cleveland).

Preliminary scaling experiments showed little additional speedup when using more than 16 CPUs, and a possible slowdown as the number of CPUs exceeded 20. However, these tests were conducted using a smallish data set, and should be repeated with a larger one. Initial tests were also conducted on Gordon vSMP nodes, which hold only 16 CPUs per motherboard; this is another possible cause of the poor scaling beyond 16 CPUs, and should be compared with scaling tests on conventional single-board, large-memory UMA machines.

4.   dayMOPS: Orbits

Orbits are used in a variety of places within dayMOPS (and nightMOPS). We fit orbits (6 parameter Keplerian orbits) to the sets of diasources which make up a track in order to determine which tracks correspond to real moving solar system objects, as the orbit fits provide much tighter constraints on the linkages than the track fits. After determining an orbit for a movingObject, we identify potential additional detections from both previous observations and future observations by predicting the positions of the movingObject from the orbit, adding those detections to the fit, and re-evaluating the orbit, through the processes of precovery and attribution. We also use orbits and their uncertainties to determine the positions and their uncertainties of known movingObject for nightMOPS.

Thus, under the general heading of 'orbit software' we actually have a variety of needs. These include:

- Ephemeris generation. This is software to generate positions, velocities, and magnitudes of moving objects at a particular time from a given orbital element distribution. This is needed for nightMOPS and for precovery and attribution.

- Orbit propagation. This is software to propagate orbital elements backwards and forwards in time; the resulting changes in the orbital elements can be minor (updating the mean anomaly, for example) but over a longer timespan can be major (changing semi-major axis and eccentricity due to the influence of other planets, for example). This is often bundled with ephemeris generation, but is not necessarily quite the same. This is needed for ephemeris generation, but may also be important for detecting duplicate movingObjects (a single movingObject discovered at two separate times during the survey).

- Initial Orbit Determination. This is software to fit a preliminary orbit to a set of detections, usually only used when there are only a few detections such as when we first discover a movingObject. This is needed for the orbit determination stage of dayMOPS.

- Differential Orbit Determination. This is software to fit a full orbit to a set of detections, usually incorporating all available observations and leveraging the initial orbit determination fit into a fit that includes error bars. Sometimes IOD and DOD are packaged together in orbit determination software, but mathematically these are usually separate processes with different assumptions on the underlying orbit. For example, IOD may assume that the detections represent an object near perihelion, while DOD may relax that assumption and try to fit for the perihelion location and mean anomaly.

Often all of these capabilities are bound together in a single distributed software package, but this is not necessarily the case. Furthermore, it may be to LSST's advantage to use different packages for different needs, if there are speed differences. For example, ephemeris generation and orbit propagation may be tasks that translate well to GPU architecture, given the repetitious and math intensive nature of the calculations, while IOD and DOD may not due to the individualized nature of each fit.

4.1. Orbit packages

At present, the number of available open-source software packages is limited. OpenOrb, by Mikael Granvik, provides Fortran95 code with limited python interfaces. OrbFit, by Andrea Milani, provides Fortran95 code only. Both of these software packages provide all the functionality above, although with varying disadvantages. There may be other open-source packages available, but these are the main two we have investigated, and seem to be the only two that provide all functionality required for all types of solar system objects.

One of the main differences between OpenOrb and OrbFit is their approach to IOD, and in particular, DOD. OpenOrb uses statistical ranging while OrbFit is based on geometric orbit fits for DOD. A extremely simplified description of statistical ranging would be: generate many possible orbits for a particular set of detections and see which one fits the observations the best. This has the advantage that it will (to the limits of the parameter space which is explored) find the best fit orbit, including being able to distinguish between NEOs and MBAs with short observational arcs. It will return a probability distribution function of all likely orbits, even if they are not connected in orbital parameter space. This makes it scientifically most accurate in calculating an orbit, and gives the best estimate of whether an object is truly an NEO or not. It has the disadvantage that it is calculating ephemerides for many possible orbits and comparing those predictions to the observed detections, to see which one 'fits the observations best'. This makes it compute-intensive, and as a result, slow. An extremely simplified description of geometric orbit fits would be: take the observed detections and fit an ellipse through those detections, using an analytic formula. This has the advantage that it is extremely fast in comparison to statistical ranging and could identify orbits well enough to recover the objects at a later time, even if the orbit determination was incorrect. It has the disadvantage that a single orbit, with (most likely) incorrect errors (because generally the error space is non-gaussian) is returned, and in particular, NEO orbits may be assigned to MBA objects at particular solar elongations. There is likely also differences in IOD, although these details are less clear (to me).

OpenOrb's code exceeds 60,000 lines in the main portion of the software, and provides

two different python libraries for interacting with this code. One is an f2py library which handles ephemeris generation (with and without errors) and orbit propgation, while another is a custom python interface (which may be out of date, depending on if API changes have occured) for IOD and DOD. OrbFit's codebase exceeds 160,000 lines, so is also not a simple program (there are multiple ways to find best options for the orbit fit, particularly for short arcs, beyond the simple ellipse). Note that the version of OrbFit being used by PS is not quite the same as the open-source version: Milani rewrote some of the code to be faster. There are no python bindings, and OrbFit interacts with data through text files (separate files for each object).

A rough comparison of the relative speed of orbit determination using each of these methods gives:

- OpenOrb 20s / track (estimates from JM) [10s for ranging (IOD) with a subset of detections, 10s LSL (DOD) with all linked detections]

- OrbFit 0.005s / track (estimates from PS)

Obviously, this difference in orbit fitting is significant. It is likely that the requirements for OpenOrb could be tuned with better understanding of the ranging and least-squares stages, but it seems unlikely that it will be as fast as OrbFit (or even within a few orders of magnitude). Beyond considerations of the speed of orbit fitting, there are also considerations of ease of use and integration with the LSST stack. This is where OrbFit is difficult, as requiring text files for each object will not scale well for the number of objects expected in LSST or for our computing platform. In addition, it would be difficult for LSST to maintain these codes independently of the original authors.

Orbit determination is performed per-track and is thus trivially parallelizable. In addition, unlike the linking phases, these algorithms require little memory overhead.

In terms of ephemeris generation, both packages appear similar. We have done some tests to determine the timing requirements for ephemeris generation with OpenOrb and find

$$\text{Time}_{10,000\,\text{objects}}(s) \approx 0.7(\frac{s}{\text{day}})(\text{Days from Orbit Epoch}) + 3.5(s) \tag{9}$$

on a macbook pro (see Figure 23). The major things to note here are that the time required to generate an ephemeris increases as the difference between the orbital epoch and the time of the requested ephemeris increases (due to the need to propagate the orbit to the time of the ephemeris), and that there is some overhead due to reading in the JPL binary files that describe the position of the Earth and other major planets and writing out the outputs. In addition, the time required to generate ephemerides for N objects scales as O(N).
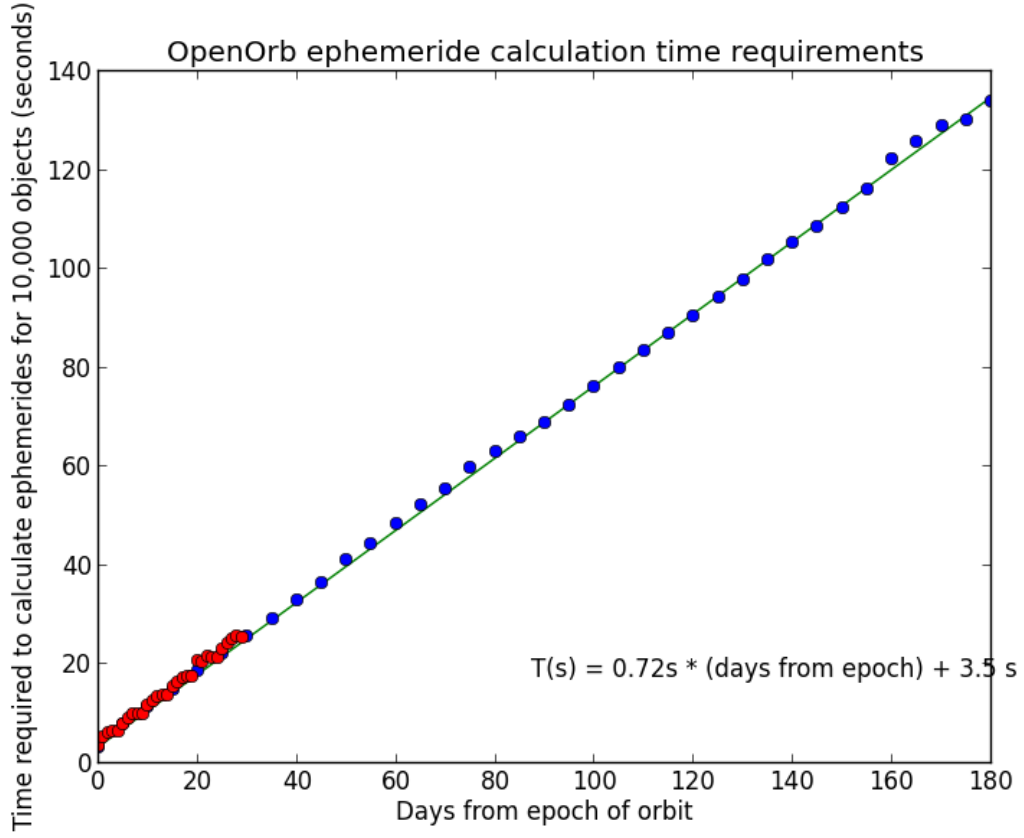
Fig. 23.—: Results of a test of the time required to generate ephemerides for 12,078 objects (scaled to 10,000 objects for the plot) using OpenOrb.

5. Precovery and Attribution

This section is intended to provide a brief overview of the requirements for precovery and attribution, along with some speculation on how these tasks may be implemented.

5.1. Attribution

Attribution is the process of adding new observations to an existing movingObject, thus increasing its observed orbital arc. This decreases the errors in the orbital parameters, generally making the object more useful for dynamical modeling or studying orbital distributions of populations and making future ephemeris predictions for the object more accurate. These additional observations are particularly useful when the orbital arc is short.

Attribution could take place by adding single detections within a night, if the ephemeris prediction is suitably low in error and a comparison image or template shows that no other star, galaxy or transient object is present at the predicted location. This process should be considered if the LSST cadence results in many single visits per night, or perhaps as an additional goal to fill in as many observations as possible. However, in general, it will be more reliable to extend the arc by looking for multiple observations of the same moving object within a night, so as to use not only the position but also the velocity as match criteria. This allows larger ephemeris errors to still result in a reliable identification and means that tracklets should be the basis for attribution.

The process of attribution would then go as follows:

- After the night's worth of observations, dayMOPS findTracklets phase produces tracklets.

- Ephemerides for all the currently known movingObjects are produced, at some intervals over the time span of observing.

- These ephemerides (presumably placed into some form of KD-Tree holding position and velocity information) are compared to the night's tracklets (also placed in a similar KD-Tree), and the intersecting matches are inspected further.

- For each movingObject and tracklet match, take all the detections which make up the movingObject and the tracklet and use these to attempt to fit an updated orbit; if the residuals are appropriate, then the match is considered correct.

- For correct matches, the movingObject orbit is updated, the detections are flagged as belonging to this movingObject, and the detections (and any tracklets involving those detections) are removed from the set of tracklets.

- The remaining set of tracklets are then sent onwards to linkTracklets.

The details of matching the ephemerides and the tracklets have not been worked out. The LSST case is demanding because we expect about 800 observations per night and (towards the end of the survey) 11M known movingObjects; this means it will likely be impractical to brute force things by just predicting the positions of all known movingObjects at all observational times. However, work done in nightMOPS is applicable here as well if the velocities are ignored in the first stages, and only considered when examining potential matches; if the requirement is that potential matches are close to the predicted positions in more than one visit, this essentially includes the velocity condition implicitly.

5.2. Precovery

Precovery is the process of adding old observations (that could not be identified at the time) to an existing movingObject, again increasing its observed orbital arc, although here it is 'backward' in time. An additional advantage of precovery is that it reduces the uncertainty in ephemeris predictions without waiting for additional observations, thus presumably making further attribution less time consuming as the ephemeris errors become smaller. Again, the most useful method of precovery will include multiple observations within a night.

There are many possible approaches to precovery. While attribution should be attempted for all known movingObjects as soon as tracklets are formed, precovery should only be done if a movingObject's orbit is significantly changed by adding new observations ('significantly' meaning that the ephemeris predictions move beyond the region which would have been included in any previous attempts at precovery). Precovery efforts should also be limited to a timespan where the uncertainty in ephemeris predictions permit reliable matches. These two factors suggest that precovery may be best handled on an object-by-object basis, perhaps as follows:

- Using the orbit of the movingObject, generate coarse ephemerides backward in time to the point that the uncertainty in the ephemeride predictions reaches a predetermined threshhold.

- Compare these coarse ephemerides (including the predicted magnitudes) to the location

of LSST pointings (and their measured 5σ limiting magnitudes) to determine visits where the movingObject may be visible.

- For the visits where the movingObject may be visible, retrieve diaSources which do not match other known movingObjects or Objects.

- Compare the diaSources to the ephemeris predictions for each time, looking for multiple potential matches within a night.

- Combine the potential matches and the detections which make up the movingObject, and use these to attempt to fit an updated orbit; if the residuals are appropriate the match is considered correct.

- Update the diaSource table to reflect the new movingObject associations, and update the movingObject orbit with the new parameters.

This is likely to become an iterative process; precovery is performed, additional observations are identified and orbit is updated, making further precovery possible.

A complication with both precovery and attribution is that with the additional observations, it may become clear that diaSources which were previously associated with the movingObject no longer belong (*i.e.* the residuals between the orbit predictions and the location of these diaSources becomes larger than the overall RMS). This will mean that further changes in the association of diaSources will occur, and further evaluation of the orbit may be necessary (which observations should be kept, which should be discarded?).

6. Further Development Tasks

Though the core algorithms of MOPS have been implemented in LSST-appropriate style, further research and development are needed.

6.1. Long Duration Survey Performance

Current simulations cover fairly short time periods, and therefore emphasize the problem of initial object discovery. In the course of the full survey, we expect that many detected sources will be attributed to already-discovered objects. Because initial object discovery phases are relatively expensive and ephemeris calculation is relatively fast, we expect that the resource usage of the system will decline over time, as more objects are discovered and the size of input catalogs is reduced. This expectation needs to be verified and quantified.

Attribution, precovery and Moving Object management and refinement of the Moving Object table are not yet implemented in LSST-compliant software. Developing this software should be a significant development task.

To test this software, we will need to generate simulated input catalogs which span longer time periods. Improvements in the catalog generation software at UW (which took place after most of the simulations presented in this document) should make this possible.

6.2. Including Trailing for Near-Earth-Object Searching

Near-Earth Objects tend to have the highest sky-plane velocity. This presents a significant challenge; as we increase the maximum velocity limit of our tracklet generation, the potential for mislinkage increases significantly, leading to higher numbers of tracklets and increased costs.

Fortunately, fast-moving NEOs will generate visible trails in our images. By requiring all tracklets to show trails consistent with their apparent sky-plane velocity, we expect that it will be possible to filter most false tracklet linkages, thus rendering the problem of NEO searching manageable.

The ability to filter on trailing is dependent almost entirely on our ability to correctly identify trails in images. Currently, the ability of image processing to detect trails is not well quantified. To remedy this, we will need to generate simulated images which include asteroid trails and send them to image processing; further refinement of image processing

algorithms may be neccesary.

6.3. Distributed LinkTracklets

In case the implicit memory sharing is not sufficient (say, because distributed shared memory systems do not provide adequate performance), it may be necessary to write an explicitly distributed linkTracklets. This was attempted by a CS Master's student, Matt Cleveland, working with Prof. Dave Lowenthal. The design was well-thought out but complex, leading to slow implementation. The distributed version was forked off before a variety of changes to the serial version were made, and never merged with those changes.

The distributed linkTracklets, the master node held only the tracklets of the endpoint trees, and the higher levels of the endpoint and support trees. The master node would attempt the linking algorithm on the higher levels of the tree until it reached a terminal point; it would then attempt to predict the amount of work needed to complete the linking and save the state of the searching and estimated cost to a buffer. Periodically, the work items in the buffer are distributed to worker nodes, with attention given to load distribution as well as cache issues, attempting to minimize the amount of data which must be transferred to worker nodes.

6.4. Trivial Code Changes

Reducing Memory Bloat in KD-Tree Libraries Because of the size of the data sets in MOPS, memory consumption is a frequent problem. Though this cannot necessarily be addressed exclusively through improvements in software implementation alone, the overhead could be reduced significantly.

Lack of attention to the memory size in the initial implementation of the KD-Tree library has resulted in needless memory bloat of the trees. Each node uses a series of `std::vector`s which could be replaced with pointers or C-style arrays. On a 64-bit architecture, `std::vector` has an overhead of at least 24 bytes, where pointers and fixed-size arrays have an overhead of just 8 bytes. Currently, KD-Trees use four vectors, meaning an overhead of 96 bytes per node.

Further modification could further reduce the size of KD-Tree nodes; for instance, rather than storing k in an integer, it could made a template argument so the constant is "baked in" at compile time and would not need to be stored.

Removing Critical Sections in Parallel Implementations   In all the multithreaded software (except linkTracklets), we maintain a single output vector (or set) to which all threads write. To prevent conflicts, these writes must be wrapped in critical sections. Critical sections impose synchronization costs, which may become significant when threads execute on separate boards and must communicate over the network (as in vSMP or other OS-level distributed shared memory systems).

To reduce overhead, each thread should really maintain its own output vector, which could be used without any critical section and merged later, after all worker threads have completed, as is done in linkTracklets.

6.5.   Significant Changes in CollapseTracklets

Motion Vectors   Currently, collapseTracklets parameterizes motion using location, angle, and velocity. However, for low-speed objects which have significant observational error, the angle can be affected by significant error. This means that setting a threshold for angle tolerance can be difficult; if set too low, then tracklets from slow-moving objects may not be merged, and if set too high, then tracklets from fast-moving objects may be mislinked.

This problem would likely be less severe if motion angle and velocity were replaced by per-axis velocity in RA and declination. However, after making this change, it will be necessary to develop experimentally determine some effective thresholds, which can be a time-consuming process.

Polar Distortion   When projecting the locations and motion vectors of objects to a common time, the current collapseTracklets implementation currently treats celestial coordinates as though they were planar. This is fairly effective close to the ecliptic, but near the poles it could be problematic. Fixing this should be relatively trivial, but it has not yet been done.

Exploring Parallelism and Caching of Flags   As mentioned in 2.6.2, there are several possible methods for dealing with the per-tracklet "already merged" flags. The current implementation does not explicitly address the issue, and no attempt has been made to compare various approaches and their performance.

Currently, there is no explicit caching of the "already merged" flags, and all threads modify them without regard for locking. On a true large-memory, single-board system, this should be fine: integer-sized reads should be atomic, meaning no partially-written results

could be read, and only in very unusual cases could a stale value be read. However, in systems with CC-NUMA systems, likely including vSMP systems such as SDSC's Gordon cluster, it is possible that stale reads could occur when threads from the same process execute on multiple boards.

6.6. Dealing with Near-Pole Distortion in LinkTracklets

The math used in linkTracklets to determine acceleration is almost certain to break down on near-pole cases. Further, the chi-squared probability fitting and filtering has not yet been tested heavily off the ecliptic, much less in cases of near-pole objects, and could reject true tracks at an increasing rate as it sees objects further from ecliptic.

To deal with the acceleration pruning near poles, it may be wise to modify the core piece of code to rotate pairs of nodes to near the origin at each pruning check; however, this may be too computationally costly to insert into the "hot spot" of the program. Another solution would be to abandon celestial coordinates and instead use full (x,y,z) Cartesian coordinates on a unit sphere. This will require new math be used for calculating acceleration and pruning, as well as for tree construction. It is unclear how performance will be affected by the change.

Additional evaluation is needed before it becomes clear whether changes to the higher-order fitting code and chi squared probability filter will be needed due to these geometry distrotions.

6.7. Dense and Clustered Noise

The rate of false tracklet generation increases worse-than-linearly with the density of detections. Issues with image processing can lead to dense clusters of false detections packed in a small area, which can in turn lead to very large growth in the number of false tracklets.

Additional experimentation will be needed to determine how severe this problem could be. If it becomes an issue, it may be necessary to identify regions with unusually high rates of (potentially) false detections and simply remove all detections from this region before the data is fed to MOPS. It's worth noting that PanSTARRS is implementing a technique similar to this to deal with high densities of detections.

A.   A Little History of Discovering Moving Objects

Contributed by Jeff Larsen

To provide a bit of background, the task of discovering unknown asteroids has a very lengthy history, involving human, electronic, and computerized actors.

From the beginning the primary detectable feature of an asteroid is it's motion across the sky as time progresses – which makes the underlying orbital parameters of critical relevance to the continued tracking of the object. The first asteroid, Ceres, was visually detected by Piazzi (Bode 1802) through its motions against the background star as he attempted to verify the position of a star in a published catalog. Without knowing how orbits were goverened, Piazzi's initial tracking effort involved constant repeated night-to-night observations which he was only able to maintain for a limited time due to his health and the motion of the asteroid into the daytime sky. It fell to Carl Friedrich Gauss to develop his method of orbit determination before Ceres could be recovered again thus firmly establishing the mathematics of orbits as a required prerequisite.

Optical observations had their limitations, however, and the archival record created by the application of photography to observations was of critical importance to scientific demands of repeatability. The first photographic discovery of an asteroid, (323) Brucia, was by Max Wolf in 1891 (Wolf 1892) as he recognized the non-sidereal rate trails on his photographs for the asteroids they were. Wolf became a prolific discoverer of asteroids (almost 250 total) through photography and as such developed the standard detection technique used for the next century.

Photographic sensitivity is determined to a large part through exposure time and asteroid motion to first order is a function of its distance so two main types of photographic survey methodology were used. Surveys looking for closeby and fast near-Earth asteroids (like those of Shoemaker & Shoemaker (1988)) used non-sidereal trailed motions and generally shorter exposure times. A discovered trail of any length in the and image developed in an observatory darkroom would lead to additional exposures of the asteroid being quickly acquired and the data required to secure the orbit. The second technique, useful for very slow moving asteroids that did not appear as a trailed images was to take several exposures and then manually alternate between them rapidly, thus depending on the well-developed human motion sense to discover the moving asteroids. Machines were built for this purpose, such as the blink comparator. Besides its use for stellar proper motions, this technique's most well known success was in the discovery of Pluto by Tombaugh (Tombaugh 1960). The blink comparator was useful for scientific studies of asteroids in the main asteroid belt such as the seminal Palomar-Leiden survey (van Houten et al. 1970). Keeping the exposure times

short was important to keep the asteroid images starlike so their isophotal diameter could be used inaccurate brightness calibration. This allowed for the rapid discovery of asteroids for the time: 2400 discoveries in 11 nights of observation.

The advent of the CCD was applied to asteroids early, with the long readout times (and consequential 50% duty cycle) minimized through the process of drift scannings. Gehrels and the Spacewatch Project (Gehrels et al. 1990) pioneered the use of CCD's in the detection of asteroids, making the first CCD detection of the near-Earth asteroid 1989 UP and the first discovery as well (1990 SS). Spacewatch went on to built an advanced real time asteroid motion detection program, MODP (Rabinowitz 1991). Drift scanning was made unnecessary by the advent of large format cameras used in a step-and-stare mode such as that of the NEAT project (Pravdo et al. 1999). With the introduction of custom frame-transfer CCD's and high-capacity computer processing, the LINEAR project (Stokes et al. 2000) and the Catalina Sky Survey (Larson 2007) were able to progress handily towards the Spaceguard goal.

As with photography, there are multiple techniques which can be applied to CCD images to discover their asteroids. Most asteroid detection software uses a "moving target indicator" approach in that CCD images are searched automatically for their objects who are then compiled as a detection list. By filtering out objects which did not move and searching for asteroid-like motions in the unmatched lists, motion candidates are created. However, a more exotic approach called Matched Filter Processing (Gural et al. 2005) can be applied that has several advantages. Images are coadded rapidly along hypothesized motion vectors. If the flux of an object appears to grow after coaddition, it becomes a candidate moving object with the motion vector already determined. Any technique to search for moving objects below the single-image limiting magnitude becomes computationally expensive with a large number of possible motion vectors, but has the advantage of being able to detect fainter objects in the same set of images compared to the moving target indicator approach. Variants on these techniques have been used successfully in searches for distant objects such as those in the Kuiper Belt (Gladman et al. 1998; Chiang and Brown 1999) and has been used to do NEA searches over large portions of the sky where the asteroid is uncertain but has a relatively small range of possible velocities (Gural et al. 2005).

The advent of large-format all sky surveys have radically changed the detection requirements both in terms of techniques for imagery and software, eventually leading to the PS and LSST MOPS software.

B.   About the KD-Tree Library

The findTracklets, collapseTracklets, and linkTracklets algorithms used in DayMOPS all require the use of KD-Trees for different types of data. FindTracklets needs an (RA, Dec) tree of detections, collapseTracklets needs an (RA, Dec, velocity, angle) tree of tracklets, and linkTracklets needs a specialized (RA, Dec, RA vel, Dec vel) tree of tracklets. Other "helper" tools not described in this document have been constructed using trees over various types of data (such as collections of orbits).

To suit the needs of our various algorithms, and to prepare for the possibility of new algorithms, we have created our own KD-Tree library. The design is intended to fulfill the following needs:

- Hold spatial points in arbitrary-dimensional space, with each point mapped to an arbitrary piece of non-spatial data

- Deal with spatial axes which hold real-number values

- Deal with spatial axes which hold degree or radian values on a circle

- Deal with pairs of axes which may describe points on a sphere

- Allow range searching in circular, spherical or flat Euclidean space

The `KDTree` class we have created suits all of these needs. These features are sufficient for almost all our algorithms. However, linkTracklets uses trees in unusual ways and its performance is closely related to the characteristics of the tree it uses; in order to allow linkTracklets' special needs, we also created a class called `TrackletTree` used only for link-Tracklets. Both `KDTree` and `TrackletTree` derive from a common base class `BaseKDTree` which implements memory management and other common features.

B.1.   Representing Data Items: PointAndValue Class

Most DayMOPS algorithms deal with identifying groups of data items based on their spatial location in some coordinate system. To represent a data item and its spatial location, we have created a template class called `PointAndValue`. A `PointAndValue` holds a point in an arbitrary-dimensional coordinate system, represented as a `std::vector` of `double` values. The coordinate system may be arbitrary-dimensional, and may also be heterogenous; that is, some axes may be Euclidean (having arbitrary values) but others may be circular, or two

axes may describe a sphere. The "value" may be anything - this is a templatized data type. In our code, it usually holds an integer, representing the location of a detection or tracklet in an array. Using a `PointAndValue` instance, one can represent any data object (the "value" of arbitrary type) and a location of that data object.

B.2. Tree Construction and Searching

`KDTree` instances are constructed from a `std::vector` of `PointAndValue` instances. The k value (the dimensionality of the tree) must be specified at construction-time. Each "point" vector used to build the tree must have at least k elements, though the software will allow "points" with $> k$ elements, in which case only the first k are used.

When providing the data for points used in tree construction, it is up to the user to ensure that any value intended to represent a measurement in degrees must fall along $[0, 360)$. Failure to do so will lead to an exception later.

If you wish to treat your spatial points as all Euclidean, it is possible to perform a conventional range search, which searches for all points in the tree within a given distance of a query point using `KDTree::rangeSearch`. However, if your axes use differing units, or one or more describe points on a circle, range search will not be suitable, as it does not handle wrap-around in degree units. This type of searching is provided by the library, but is not used within DayMOPS.

In order to deal with data points which may not be in a Euclidean space, the library supports rectangular (or hyper-rectangular) searches on mixtures of Euclidean and/or circular axes. A query point is provided in each axis, and a query range around that point; any point which is within the query range of the query point in each axis is returned. This is suitable when searching, for example, for motion vectors, which have a velocity and angle of motion; specify a range of velocities, and a range of angles, and the tree library will find motion vectors which fall within the given range. Wraparound will be handled intelligently (that is, the code will recognize that .1 and 359.9 degrees are separated by .2 degrees, not 359.7.) To use this type of searching, use the `KDTree::hyperRectangleSearch` method. Note that it will be necessary to inform the tree of which axes are Euclidean, and which are circular. Currently, the only supported units for circular coordinates are degrees, and degree measures must fall along $[0, 360)$. This is the type of searching used in the `collapseTracklets` implementation, which searches for similar points in (RA, Dec, velocity and motion angle). Unfortunately, this type of searching considers each axis independently, which can be problematic when dealing with a pair of axes which describe points on a sphere, where polar

distortions may occur.

To deal with coordinates on a sphere and intelligently account for both wraparound and polar distortion, the library provides the function `KDTree::RADecRangeSearch`. This function performs a range search on the surface of a sphere; it also allows rectangular searching of other axes if needed. The types of the axes should be specified at searching time as in `KDTree::hyperRectangleSearch`, if any. This is the search function used by findTracklets, which represents points as simple RA, Dec coordinates. It would probably be wise to change collapseTracklets to use this function as well, though this has not yet been done.

B.3. TrackletTree

The linkTracklets algorithm uses KD-Trees in an unusual fashion, and is highly sensitive to their construction. It also requires the spatial regions held by each tree node to be extended to account for error bars on the tracklets. For these reasons, linkTracklets does not use the normal `KDTree` class used by other algorithms, but a sibling class called `TrackletTree`. These classes share the common ancestor `BaseKDTree`, which handles memory management, but otherwise they share relatively little. `TrackletTree` calculates the extents of the nodes differently than `KDTree`, and it implements no range searching.

`KDTree` and `TrackletTree` hold references to the head of the actual tree nodes, implemented by `KDTreeNode` and `TrackletTreeNode`. In `KDTree` these child nodes are not visible to the user; all communication is done with the `KDTree`, which in turn communicates with the `KDTreeNode`s. This allows easier memory management, as an outside tool cannot hold a reference to a dynamically-allocated child. However, in linkTracklets these children must be visible to linkTracklets, as it explicitly traverses the tree.

`TrackletTreeNode` also has a few methods for studying performance: `TrackletTreeNode::addVisit` and `TrackletTreeNode::getNumVisits` can be used to count the number of times a node is examined by linkTracklets. Eventually, it may be wise to remove these in order to conserve memory.

B.4. BaseKDTree and Memory Management

`KDTree` and `TrackletTree` represent a whole tree, not the individual nodes which make up the tree. `KDTree` then provides an interface to the querying of the tree, while `TrackletTree` provides accessors allowing an outside class to see the actual tree nodes.

Both classes derive from `BaseKDTree` which handles the mundane work of a C++ class: construction, copying, and detruction, etc. `BaseKDTree` handles copying of a tree by incrementing a refcount on the child nodes; once those nodes hit a refcount of zero, then the nodes are deleted. This approach works well, provided no outside class holds on to references to a tree's nodes after destroying the tree itself.

B.5.   Needed Improvements

The KD-Tree nodes at present use quite a bit of memory because they use `std::vector` where a set of pointers or C-style array would probably be better-suited. This is particularly noteworthy in the case of `TrackletTreeNode`, since trees given to linkTracklets can be very large.

REFERENCES

Bentley, J. 1975, Commun. ACM, 18, 509

Denneau, Jr., L., Kubica, J., & Jedicke, R. 2007, in Astronomical Society of the Pacific Conference Series, Vol. 376, Astronomical Data Analysis Software and Systems XVI, ed. R. A. Shaw, F. Hill, & D. J. Bell, 257–+

Granvik, M. 2007, PhD thesis, University of Helsinki, Helsinki, Finland

Granvik, M., Virtanen, J., Oszkiewicz, D., & Muinonen, K. 2009, Meteoritics and Planetary Science, 44, 1853

Grav, T., Jedicke, R., Denneau, L., Chesley, S., Holman, M. J., & Spahr, T. B. 2011, PASP, 123, 423

Kubica, J. 2005, PhD thesis, Robotics Institute, Carnegie Mellon University, Pittsburgh, PA

Kubica, J., Moore, A., Connolly, A., & Jedicke, R. 2005, in Proceedings of the eleventh ACM SIGKDD international conference on Knowledge discovery in data mining, KDD '05 (New York, NY, USA: ACM), 138–146

Milani, A., Gronchi, G. F., Vitturi, M. D., & Knežević, Z. 2004, Celestial Mechanics and Dynamical Astronomy, 90, 57

Milani, A., et al. 2006, in IAU Symposium, Vol. 229, Asteroids, Comets, Meteors, ed. L. Daniela, M. Sylvio Ferraz, & F. J. Angel, 367–380

REFERENCES

Bode, J. E. 1802, Berlin : In der Himburgischen Buchhandlung, 1802.

Chiang, E. I. and Brown, M. E. 1999, AJ, 118, 1411

Gehrels, T., McMillan, R. S., Scotti, J. V., & Perry, M. L. 1990, CCDs in astronomy, 8, 51

Gladman, B. and Kavelaars, J. J. and Nicholson, P. D. and Loredo, T. J. and Burns, J. A. 1998, AJ, 116, 2042

Gural, P. S., Larsen, J. A., & Gleason, A. E. 2005, AJ, 130, 1951

Larson, S. 2007, IAU Symposium, 236, 323

Pravdo, S. H., Rabinowitz, D. L., Helin, E. F., et al. 1999, AJ, 117, 1616

Rabinowitz, D. L. 1991, AJ, 101, 1518

Shoemaker, C. S., & Shoemaker, E. M. 1988, NASA Tech. Memo., NASA TM-4041, p. 52 - 54, 4041, 52

Stokes, G. H., Evans, J. B., Viggh, H. E. M., Shelly, F. C., & Pearce, E. C. 2000, Icarus, 148, 21

Tombaugh, C. W. 1960, S&T, 19, 264

van Houten, C. J., van Houten-Groeneveld, I., Herget, P., & Gehrels, T. 1970, A&AS, 2, 339

Wolf, M. 1892, Astronomische Nachrichten, 129, 337